UNIVERSIDAD COMPLUTENSE DE MADRID

FACULTAD DE CIENCIAS QUÍMICAS

TESIS DOCTORAL

Desarrollo de nuevos compuestos inspirados en la microbiota para la validación de la proteína NPM1 como diana terapéutica de la Leucemia Mieloide Aguda

Development of new microbiota-inspired compounds for the validation of NPM1 protein as a therapeutic target for Acute Myeloid Leukemia

MEMORIA PARA OPTAR AL GRADO DE DOCTOR

PRESENTADA POR

Anabel Sánchez Merino

DIRIGIDA POR

Maria Luz López Rodríguez
Bellinda Benhamú Salama
Maria del Henar Vázquez Villa

UNIVERSIDAD COMPLUTENSE DE MADRID

FACULTAD DE CIENCIAS QUÍMICAS

DEVELOPMENT OF NEW MICROBIOTA-INSPIRED COMPOUNDS FOR THE VALIDATION OF NPM1 PROTEIN AS A THERAPEUTIC TARGET FOR ACUTE MYELOID LEUKEMIA

DESARROLLO DE NUEVOS COMPUESTOS INSPIRADOS EN LA MICROBIOTA PARA LA VALIDACIÓN DE LA PROTEÍNA NPM1 COMO DIANA TERAPÉUTICA DE LA LEUCEMIA MIELOIDE AGUDA

Memoria para optar al Grado de Doctor presentada por:

Anabel Sánchez Merino

Directoras:

Dra. Maria Luz López Rodríguez

Dra. Bellinda Benhamú Salama

Dra. Maria del Henar Vázquez Villa

MADRID, 2024

UNIVERSIDAD COMPLUTENSE DE MADRID

FACULTAD DE CIENCIAS QUÍMICAS

PROGRAMA DE DOCTORADO EN QUÍMICA ORGÁNICA

DEVELOPMENT OF NEW MICROBIOTA-INSPIRED COMPOUNDS FOR THE VALIDATION OF NPM1 PROTEIN AS A THERAPEUTIC TARGET FOR ACUTE MYELOID LEUKEMIA

DESARROLLO DE NUEVOS COMPUESTOS INSPIRADOS EN LA MICROBIOTA PARA LA VALIDACIÓN DE LA PROTEÍNA NPM1 COMO DIANA TERAPÉUTICA DE LA LEUCEMIA MIELOIDE AGUDA

Memoria para optar al Grado de Doctor presentada por:

Anabel Sánchez Merino

Directoras:

Dra. Maria Luz López Rodríguez

Dra. Bellinda Benhamú Salama

Dra. Maria del Henar Vázquez Villa

MADRID, 2024

“Nothing in life is to be feared,
it is only to be understood.”
Marie Curie

El presente trabajo ha sido realizado en el Laboratorio de Química Médica del Departamento de Química Orgánica de la Facultad de Ciencias Químicas de la Universidad Complutense de Madrid, bajo la supervisión de las ***Prof. María Luz López Rodríguez***, ***Bellinda Benhamú Salama*** *y* ***María del Henar Vázquez Villa****, a quienes deseo agradecer su cálida acogida en el grupo y la confianza depositada en mí para llevar a cabo este proyecto. Igualmente, les agradezco las numerosas enseñanzas impartidas y su atenta disposición durante todos estos años.*

Asimismo, quiero expresar mi agradecimiento:

A las Prof. Mar Martín-Fontecha Corrales y Silvia Ortega Gutiérrez por toda su ayuda en el laboratorio y en cualquier gestión a lo largo de la tesis.

A Lola, Elena, Marga y Ángel del Centro de Apoyo a la Investigación (CAI) de Resonancia Magnética Nuclear y a Estefanía y Gabriel del CAI de Masas de la UCM, por su ayuda y buenos consejos. También, a la Prof. Ángeles Canales por su supervisión en mis experimentos de RMN con la proteína.

Al Dr. Miguel Gallardo Delgado del grupo de Tumores Hematológicos del CNIO por su asesoramiento y guía en toda la parte biológica de la tesis desde el inicio. Igualmente, me gustaría agradecer tanto a él como a todo su grupo por incluirme como una más en todas mis visitas y responder mis miles de preguntas. Especialmente a Michel, cuyo trabajo y esfuerzo han sido esenciales para poder lograr el objetivo de mi tesis.

A la Prof. Irene Díaz-Moreno y su grupo del cicCartuja (Sevilla), por su colaboración en los experimentos de calorimetría.

To Prof. Lee JungHo from the NMR Lab at Seoul National University (South Corea), for accepting me in his lab for a short research stay and for participating as one of my thesis reviewers. Also, I would like to thank his research group for making me feel at home on the other side of the world. And special thanks to JongHyuk, whose kindness and patience with me were truly unmatched.

A todos los compañeros del departamento: Patri & Sergio, Nazarios, Sierras, los de Matías… porque sois los que hacéis que este departamento merezca la pena.

A mi grupo, mi familia MedChemLab. A los que terminaron antes, a los que pasaron brevemente y a los que siguen. A Jon, por acompañarme en este camino desde los primeros meses, con su apoyo y su Spotify. A Román, por alegrarme los días con sus bromas y su forma de ser. A Iván, por ser mi compañero en el apasionante mundo de la microbiota, las reacciones en cascadas y mi primer profesor de biología. A Vero, por ser mi apoyo constante en el laboratorio; sin ella, habría sido imposible mantener el orden. A Andrea, por sus enseñanzas durante mis primeros meses en el laboratorio y sus valiosos consejos como experta del MedChem. A Paola, por su originalidad y su inestimable ayuda durante mi experiencia como "resonera". A Marce y Bea, por su paciencia como biólogos en un laboratorio de químicos. A Dani y Patri, por su entusiasmo, que espero no pierdan

hasta el final de sus tesis. Y porque Taylor Swift siempre lo dice mejor: "I had the time of my life fighting dragons with you; Long live".

A Esme, lliriana madrilenya, per totes les nostres quedades de compres, frikisme i reflexions sobre la vida, per les d'aquests anys i per moltes més, ja siga a Madrid, Corea o al nostre benvolgut poble.

A les meus amigues Aida, Paula i Laura, amb les que començí la meua vida com a química, per estar sempre al meu constat pesi a distancia i la "vida adulta".

Y per últim i, en este cas, mes important a la meua família. Als meus tios, cosines y abuela, que encara no acabem de entendre el meu treball, sempre estan orgullosos de mi. Als meus pares, per ajudar-me en tot moment, sense importar el que fora i lo que els costara a ells. I a la meua germana, Lorena, per ser la força que me ajuda ser sempre millor.

Muchas gracias a todos por apoyarme y hacer posible la finalización de este trabajo.

TABLE OF CONTENTS

ABBREVIATIONS AND ACRONYMS

Throughout this manuscript, abbreviations and acronyms recommended by the American Chemical Society in the Organic Chemistry and Medicinal Chemistry areas have been employed (revised in the *Journal of Organic Chemistry* and *Journal of Medicinal Chemistry* in July 2024: *https://pubs.acs.org/userimages/ContentEditor/1218717864819/joceah_abbreviations.pdf* and *http://pubsapp.acs.org/paragonplus/ submission/jmcmar/jmcmar_abbreviations.pdf)*. In addition, those indicated below have been used:

ACN	Acetonitrile
AcOH	Acetic acid
ATCC	American type culture collection
CAI	Centro de apoyo a la investigación
CFU-E	Colony formation unit-erythroid
CNIO	Centro Nacional de Investigaciones Oncológicas
CSC	Cancer stem cells
DIPEA	*N*,*N*-Diisopropylethylamine
DMEM	Dulbecco's modified eagle medium
EDC	*N*-(3-Dimethylaminopropyl)-*N*'-ethylcarbodiimide
EtOAc	Ethyl acetate
EtOH	Ethanol
FBS	Fetal bovine serum
IDR	Intrinsically disordered region
ITC	Isothermal titration calorimetry
IVIS	*In vivo* imaging system
HLM	Human liver microsome
HSC	Hematopoietic stem cell
k_D	Dissociation constant
HRPTEpiC	Human renal proximal tubule epithelial cells
MeOH	Methanol
MLM	Mouse liver microsome
MTT	3-(4,5-Dimethyl-2-thiazolyl)-2,5-diphenyl-2*H*-tetrazolium bromide
MW	Microwave

NES	Nuclear export signal
NLS	Nuclear localization signal
NoLS	Nucleolar localization signal
NPM1	Nucleophosmine 1
NPM1^{mut}	*NPM1* gene mutation
PDX	Patient derived xenograft
PrSc	Privilege scaffolds
qPCR	Quantitative polymerase chain reaction
RED	Rapid equilibrium dialysis
STD	Saturation-transfer difference
UCM	Universidad Complutense de Madrid
WB	Western blot
WST-1	4-[3-(4-Iodophenyl)-2-(4-nitrophenyl)-2*H*-5-tetrazolio]-1,3-benzene disulfonate, monosodium salt
XPO1	Exportin 1 protein

RESUMEN

DESARROLLO DE NUEVOS COMPUESTOS INSPIRADOS EN LA MICROBIOTA PARA LA VALIDACIÓN DE LA PROTEÍNA NPM1 COMO DIANA TERAPÉUTICA DE LA LEUCEMIA MIELOIDE AGUDA

Este apartado se ha eliminado en esta versión por confidencialidad.

SUMMARY

DEVELOPMENT OF NEW MICROBIOTA-INSPIRED COMPOUNDS FOR THE VALIDATION OF NPM1 PROTEIN AS A THERAPEUTIC TARGET FOR ACUTE MYELOID LEUKEMIA

This section has been suppressed in this version due to confidentiality.

INTRODUCTION

1. INTRODUCTION

Despite early diagnosis and the development of new treatments, many patients with acute myeloid leukemia (AML) continue to fail therapy, resulting in relapses and more aggressive cancers with poor prognosis.[1] AML is a challenging hematological malignancy characterized by a wide range of genetic alterations (Figure 1) that play a significant role in patients´ prognosis and response to treatment.[2] Therefore, the development of new therapies targeting critical genetic mutations affecting AML patients is of great importance to achieve effective treatments. In this regard, mutations in the nucleophosmine 1 gene (*NPM1*^{mut}) represent the most common genetic alteration found in AML patients and *NPM1*^{mut} AML has been recognized as a distinct leukemia entity in the classification of myeloid neoplasms by both the International Consensus Classification and the World Health Organization.[3-5] This mutation affects the entire leukemic cell population, including CD34^{+} stem cells,[6] and is frequently associated with mutations in the *FLT3* or *DNMT3A* genes, which are related to a negative prognosis and a high relapse rate.[7,8] While patients with the *NPM1* mutation have a high rate of complete remission, almost 50% relapse within the first few years.[9]

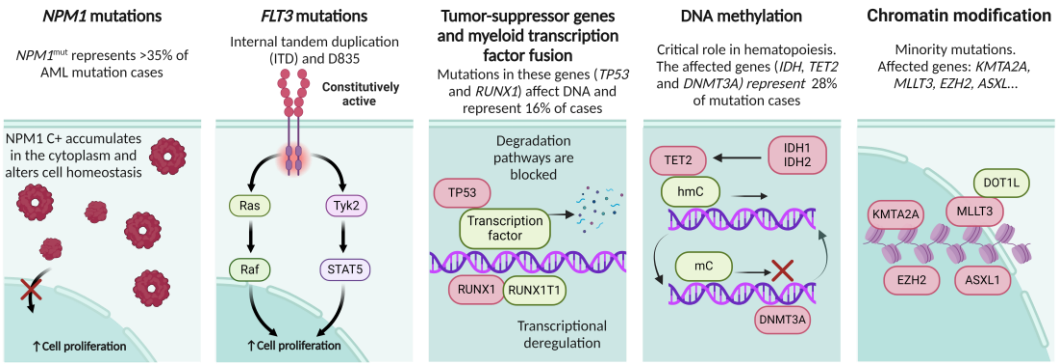

Figure 1. Schematic representation of the most frequent AML mutations and their implications. NPM1 C+: mutant NPM1 protein.

1.1.Nucleophosmine (NPM1) protein and its involvement in acute myeloid leukemia (AML)

NPM1 gene encodes for the multifunctional nuclear protein nucleophosmine 1 (NPM1) able to shuttle between the nucleolus and the cytoplasm and, as a result, involved in several key steps of the cell cycle such as centrosome duplication, ribosome biogenesis, DNA repair, histone chaperoning or liquid-liquid phase separation in the nucleolus.[10,11]

The sequence of NPM1 contains 294 amino acids that can be divided in three parts: the N-terminal domain (residues 1 to 120), the intrinsically disordered region (IDR) with two main acidic segments (residues 120 to 240), and the C-terminal domain (residues 240 to 294) (Figure 2).[12]

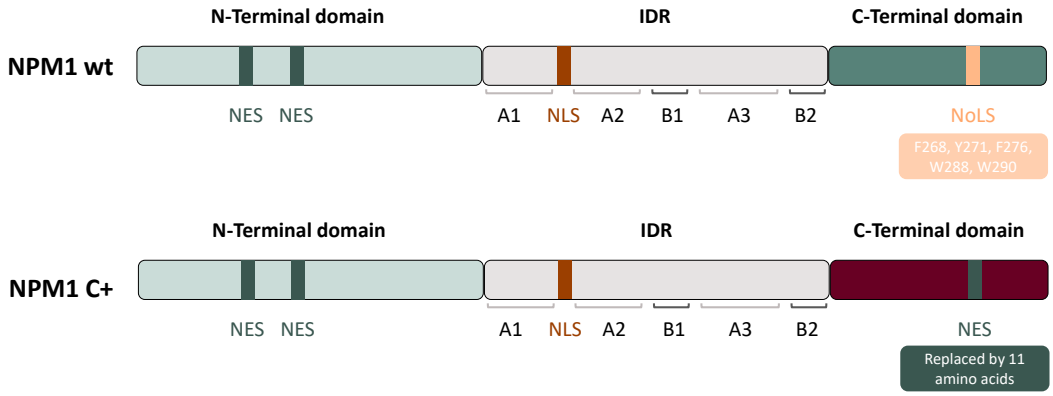

Figure 2. Schematic structure of NPM1 wt and NPM1 C+ (mutant protein) for comparison. NPM1 wt and NPM1 C+ share the same structure, differing only in the C-terminal domain nucleolar localization signal (NoLS) that is replaced by a nuclear export signal (NES). The nuclear localization signal (NLS) is maintained.

The N-terminus, the most conserved region in all isoforms and structured in eight anti-parallel β-sheets forming a barrel, is responsible for the oligomerization of NPM1 and its interaction with other proteins, such as ARF that negatively regulates cell growth. The positively charged surface on this region allows the protein to form a stable pentamer, which is known to be the most stable conformation of NPM1 (Figure 3A).[10,12,13] Furthermore, the two pentamers can interact to form a decamer, in which each monomer of the pentameric ring comes into contact with a single monomer of the other pentamer. The pentameric NPM1 can engage in different interactions through its charged regions and lead to liquid-liquid phase separation under crowded conditions modulated by ionic strength.[14] In addition, the N-terminal domain contains two nuclear export signals (NES) that enable the shift of the protein to the cytoplasm. The IDR, which contains a nuclear localization signal (NLS), is involved in the binding of the protein to histones and plays an important role in its chaperone activity. The function of the IDR is mediated by two highly acidic segments interspersed with two short basic regions (Figure 2).[14,15] As for the C-terminal domain, it is folded into three α-helices, stabilized by five hydrophobic residues

(F268, Y271, F276, W288, W290) on the inside of the formed structure and charge residues on the outside (Figure 3B). This structure is crucial for the correct activity of NPM1, as it is the part of the protein that interacts with the G-quadruplex of ribosomal DNA.[16,17] In addition, the C-terminus contains a nucleolar localization signal (NoLS) that enables the protein to shuttle back into the nucleolus.

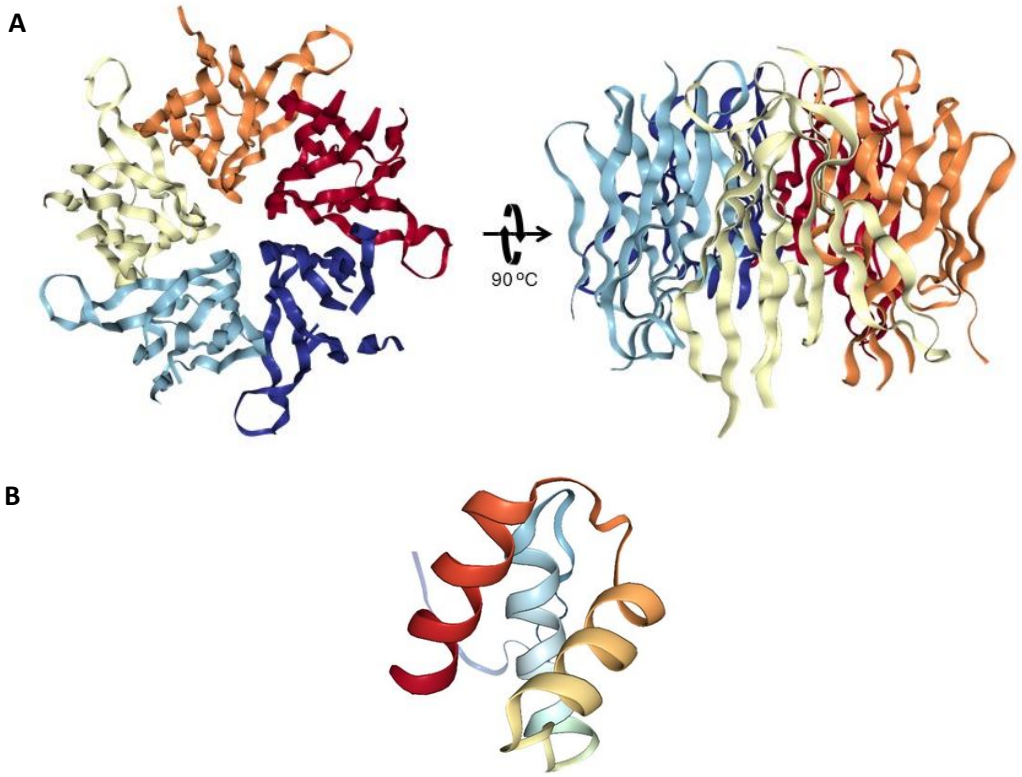

Figure 3. 3D structure of NPM1 domains. (A) Pentameric form of the N-terminus of the NPM1 model from the pdb structure 8as5.[12] (B) Three α-helix bundle of the C-terminus of the NPM1 wt model from the pdb structure 2llh.[16] Image created using NGL Viewer.[18]

Interestingly, one-third of AML patients carry an *NPM1*^{mut} that encodes for an aberrant protein, NPM1 C+ (Figure 2).[19-21] The various alterations, which typically involve the insertion of four new nucleotides in different exons of *NPM1*, result in the replacement of the final seven amino acids with an eleven-residue sequence lacking the two tryptophan residues (W288 and W290) that encode for a NoLS.[17] To date, over 50 different mutations have been documented.[22,23] However, in most cases the mutation occurs in exon 12, with the mutant A being the most prevalent variant observed in over 70% of patients (Table 1).

Table 1. Most representative cases of *NPM1*^{mut} and effect on the amino acid sequence of the protein C-terminus.

Mutant (frequency, %)	**Nucleotide sequence**	**Protein sequence** (from 286 aa)
Wilde type	GATCTCTG____GCAGTGGAGGAAGTCTCTTTAAGAAAATAG	-DLWQWRKSL
Mutant A (72-80)	GATCTCTG***TCTG***GCAGTGGAGGAAGTCTCTTTAAGAAAATAG	-DLCLAVEEVSLRK
Mutant B (8-12)	GATCTCTG***CATG***GCAGTGGAGGAAGTCTCTTTAAGAAAATAG	-DLCMAVEEVSLRK
Mutant C (<1)	GATCTCTG***CCTG***GCAGTGGAGGAAGTCTCTTTAAGAAAATAG	-DLCLAVEEVSLRK
Mutant D (3-7)	GATCTCTG***CCTG***GCAGTGGAGGAAGTCTCTTTAAGAAAATAG	-DLCLAVEEVSLRK
Mutant E (<1)	GATCTCTGGCAGT***CTCTTGCCC***AAGTCTCTTTAAGAAAATAG	-DLWQSLAQVSLRK
Mutant F (<1)	GATCTCTGGCAGT***CCCTGGAGA***AAGTCTCTTTAAGAAAATAG	-DLWQSLEKVSLRK
Mutant I (<1)	GATCTCTG***CAGA***GCAGTGGAGGAAGTCTCTTTAAGAAAATAG	-DLCRAVEEVSLRK
Mutant J (<1)	GATCTCTG***CTTG***GCAGTGGAGGAAGTCTCTTTAAGAAAATAG	-DLCLAVEEVSLRK
Mutant K (<1)	GATCTCTG***TATG***GCAGTGGAGGAAGTCTCTTTAAGAAAATAG	-DLCMAVEEVSLRK

In all variants, changes in the amino acid sequence of the NPM1 protein entail the same modifications: the loss of the NoLS, the addition of an NES (a leucine-rich section), and the unfolding of the characteristic structure of the C-terminal region, which is no longer stable.[24] This makes the mutant NPM1 C+ more prone to be exported to the cytoplasm by exportin 1 (XPO1) and unable to return to the nucleolus, resulting in the accumulation of the protein in the cytoplasm (Figure 4). Despite the altered structure, the aberrant protein is still functional and able to interact with other proteins and even aggregate with NPM1 wt in the pentameric form. Under normal conditions, NPM1 modulates stress response and growth suppression by binding and stabilizing p53 tumor suppressor protein in the nucleoplasm, and inhibiting MDM2 promoting growth arrest. It also stabilizes ARF in the nucleolus, where this protein interacts with MDM2, further preventing p53 inhibition. However, when the mutation occurs, NPM1 C+ sequesters ARF to the cytoplasm,[25] reducing its stability and causing its degradation. As a result, p53 is degraded by MDM2, blocking apoptosis in the cell. Additionally, NPM1 C+ binds and delocalizes FBWX7 tumor suppressor to the cytoplasm, which also leads to its degradation. Consequently, c-Myc oncoprotein levels increase, promoting growth and proliferation.[26] All the alterations in the cell homeostasis (Figure 4) by this still functional but misplaced NPM1 have been linked to AML leukemogenesis.[27-30]

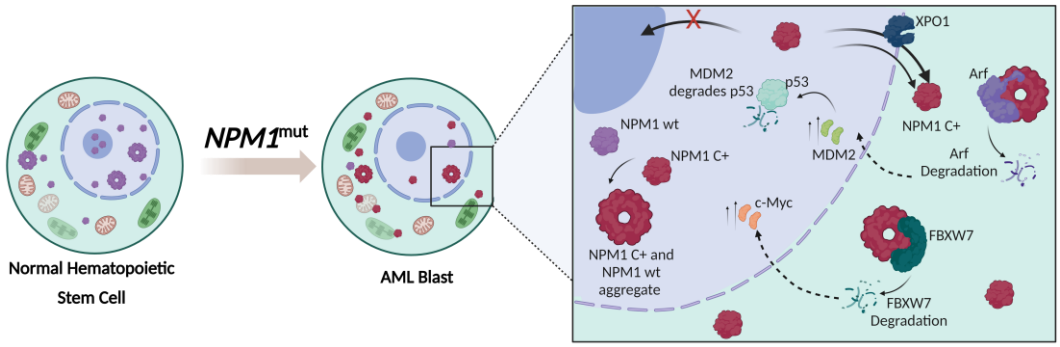

Figure 4. Schematic representation of the phenotype in normal hematopoietic cells and in cells with *NPM1*^{mut}. Molecular signaling pathways of NPM1 C+ in AML.

1.2.Current therapies and new strategies for *NPM1*^{mut} AML treatment

Standard therapies for *NPM1*^{mut} AML currently involve induction chemotherapy with or without FLT3 protein inhibitors, followed by consolidation therapy with high-dose cytarabine, and possibly allogeneic stem cell transplantation in the first complete remission.[31] Other therapies with venetoclax, an inhibitor of the anti-apoptotic protein BCL-2, combined with low-dose cytarabine or azacitidine have also proven to reduce or eliminate measurable residual disease (remaining number of leukemic cells).[32] However, despite the remarkable advances in the treatment of this pathology, about half of the patients still die due to disease progression. Thus, there is a need for new therapeutic strategies. In light of recent advances in the understanding of the genomic alterations associated with AML, new approaches targeting each of the different mutations are being developed.[33,34]

In the context of new therapeutic opportunities for *NPM1*^{mut} AML, the different strategies to target NPM1 protein with small molecules include interfering with the aberrant NPM1 C+ transport, inducing nucleolar stress in *NPM1*^{mut} cells, decreasing protein levels by the proteasome, targeting NPM1 pathway proteins or modulating NPM1 directly.[35-37] On going clinical trials are summarized in Table 2 and representative cases are described in the following.

Table 2. Molecules in clinical trials for the treatment of *NPM1*^{mut} AML.

DRUG CANDIDATE	TARGET	CLINICAL TRIAL
KPT-8602 (Eltanexor)	XPO1 inhibition (NPM1 export inhibition)	NCT02649790 (Phase I/II)
KPT-330 (Selinexor)	XPO1 inhibition (NPM1 export inhibition)	NCT02093403 (Phase I) NCT02249091 (Phase II) NCT02088541 (Phase II) NCT01607892 (Phase I) NCT03955783 (Phase Ib)
Actinomycin D	Nucleolar stress induction	Phase II pilot study[a] 2014-000693-18 (Phase II) 2014-003490-41 (Phase II)
ATO	Proteasomal degradation	NCT04689815
SNDX-5613 (Revumenib)	MLL-Menin protein–protein interaction inhibition	NCT04065399 (Phase I/II recruiting)[b]
KO-539	Menin inhibition	NCT04067336 (Phases I/II recruiting)
JNJ-75276617	MLL-Menin protein–protein interaction inhibition	NCT04811560 (Phase I)
DS-1594b	Menin inhibition	NCT04752163 (Phase I/II)
BMF-219	Menin inhibition	NCT05153330 (Phase I)

[a]44% efficacy (n=9). [b]30% efficacy.

As mentioned before, NPM1 is located mainly in the nucleus, but when the mutation occurs the protein accumulates in the cytoplasm, disrupting the normal functions of the cells. One way to prevent this mislocation is to target XPO1, which mediates NPM1 export to the cytoplasm. Among others, the compound KPT-8602, a selective XPO1 inhibitor also known as eltanexor,[38,39] has shown great anti-leukemic efficacy in preclinical animal models of hematological malignancies and is currently being evaluated in phase I/II clinical trials (Table 2).

In terms of nucleolar stress-inducing therapies, actinomycin D, a polypeptide antibiotic, has shown an encouraging outcome in a phase II pilot study of relapsed *NPM1*^{mut} AML patients, in which more than 40% of patients achieved complete remission (Table 2).[40] Despite the incomplete understanding of its mechanism, this molecule is believed to target mitochondria-primed cells.[41] Hence, its capacity to induce oxidative stress appears to be a promising approach, suggesting the potential value of considering other drugs that cause nucleolar stress, such as anthracyclines, for the treatment of this disease.

Another widely used strategy is proteasomal degradation. Notable among compounds with this activity is arsenic trioxide, known as ATO,[42] which has exhibited antitumor activity due to a selective capacity to induce proteasomal degradation of NPM1 C+, leading to cell apoptosis (Table 2). The combination of ATO with all-trans retinoic acid

(ATRA) is already used in the treatment of acute promyelocytic leukemia, a subtype of AML (NCT02688140).

Currently, one of the most predominant strategies employed is targeting the menin protein, which disrupts the complex menin-MLL1 or the interaction of this protein with oncogenic MLL fusion proteins. Inhibition of the complex formation alters the binding of MLL1 to a subset of target genes, including homeobox gene *MEIS1*, resulting in the loss of transcriptional activity and growth arrest.[43] A number of small molecules are currently in advanced preclinical development and several novel candidates are in clinical trials (Table 2).[44-46] Among them SNDX-5613, also known as revumenib, has successfully passed clinical phase I in patients with *NPM1*^{mut} AML with and without other genetic alterations such as *FLT3*. In this phase, the maximum tolerated dose of SNDX-5613 has been established and an initial efficacy assessment has been conducted, allowing the new drug candidate to advance to phase II.[47]

1.3.Targeting NPM1 modulation

Direct targeting of the NPM1 structure represents a highly efficient mechanism for modulating NPM1 levels or its interactions with other proteins. However, the number of molecules, and of small molecules among them, that interact directly with NPM1 is scarce and none of them have reached clinical development for the treatment of AML.[48,49] Nevertheless, this strategy has shown promise for further development and represents today an opportunity to validate NPM1 as a therapeutic target.

To date different approaches have been contemplated to target NPM1 modulation.[35,50] For instance, targeting the oligomerization of NPM1 could be an interesting mechanism. By inhibiting the formation of the stable pentamer, the protein can be destabilized, leading to its degradation. Alternatively, preventing oligomerization could result in an alteration of the major functions of the NPM1 pentameric unit, such as protein-protein interactions of the oligomer. Another potential option is to influence the folding of NPM1, specifically the aberrant C-terminal domain of NPM1 C+. In this scenario, stabilization of the unfolded terminus could result in the relocation of the protein to the nucleus, thereby preventing the protein from engaging in undesirable interactions within the cytoplasm. So far, different molecules have been identified as modulators of NPM1 through one of the above-mentioned mechanisms (Figure 5).

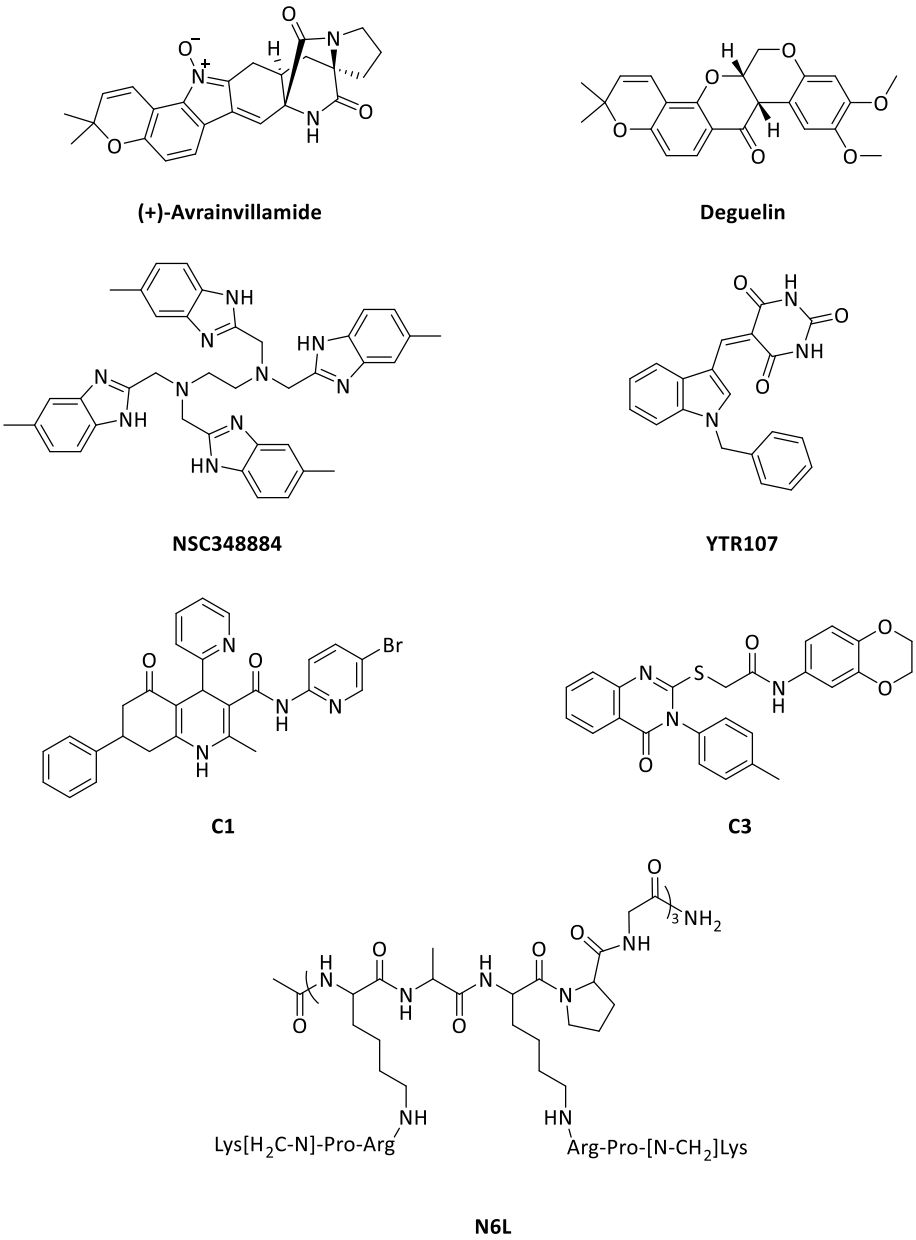

Figure 5. Chemical structure of compounds targeting NPM1 modulation.

Within this group of small molecules is (+)-avrainvillamide (Figure 5). This natural product is able to form a thioether bond with Cys275 present in the C-terminal domain of NPM1.[51,52] *In vitro* experiments show a stronger binding to the C-terminus of NPM1 C+, probably due to the unfolded structure that makes Cys275 more available. The interaction of (+)-avrainvillamide with the protein has been extensively studied and it is also known to be able to partially relocate the aberrant protein to the nucleus, acting like a substitute of the NoLS. Moreover, the natural product has shown efficacy in the nanomolar range in several AML cell lines with both NPM1 wt and NPM1 C+ (NB4, HL-60, MV4-11, OCI-AML3, MOLM13).[53]

Another natural product believed to act on NPM1 is deguelin (Figure 5). The compound has shown the ability to downregulate NPM1 C+ protein levels and induce apoptosis in OCI-AML3 cells (IC_{50} = 1.49 μM) without affecting NPM1 wt expression levels.[54] Although several studies indicate deguelin is a protein kinase inhibitor and have related its apoptotic effect to this interaction,[55] its mechanism in *NPM1*^{mut} AML remains unclear, since the compound is able to induce cell differentiation in *in vitro* and *in vivo* models with NPM1 C+.[56]

In addition to these natural products, some synthetic compounds that interact with NPM1 are also known. One of the first of them is NSC348884 (Figure 5), identified by virtual screening using a pharmacophore model developed by analyzing the hydrophobic surface of NPM1, which allows its oligomerization.[57] In the initial assessments, the compound showed good efficacy (IC_{50} = 1-10 μM) in various skin (Colo 16 and SRB-12) and gastric (MKN-28 and SNU-484) cancer cell lines. In the case of *in vitro* AML models, it exhibited heightened efficacy in cells expressing NPM1 C+ (OCI-AML3). Since then, the interaction of NSC348884 with NPM1 has been extensively investigated, and it was postulated that the compound acts on NPM1 by inhibiting its oligomerization, resulting in elevated levels of p53 and apoptosis.[58] However, recent studies have challenged this mechanism, indicating that the apoptotic effect of NSC348884 is not mediated by inhibiting NPM1 oligomerization, but appears to affect cell surface adhesion.[59] Nevertheless, the compound is still in preclinical development and further studies are needed to definitely elucidate its mechanism.

Another noteworthy compound is YTR107 (Figure 5), which has also demonstrated its capacity to impede NPM1 oligomerization.[60,61] It is a radiosensitizing compound that interferes with DNA damage repair mechanisms, sensitizing different tumor cell lines, mostly related to colon or lung cancer, to radiation. Due to its promising results, the development of new YTR107 analogues with enhanced activity is underway.[62,63] Some of them have been able to reduce cell growth to 50% in the micromolar range in different *in vitro* cancer models, including several leukemia cell lines (CCRF-CEM, HL-60, K564, MOLT-4, RPMI-8226, SR).

Recently, compounds reported as C1 and C3 (Figure 5) were identified as stabilizers of the C-terminus of NPM1 C+, in a high-throughput screening using differential scanning fluorimetry.[64] Both compounds were found to restore the nucleolar localization of the mutant protein, thereby enabling partial recovery of NPM1 normal functions. However, no efficacy assays have been conducted for the treatment of AML with these compounds. Consequently, further studies are necessary to assess their therapeutic potential.

A borderline small molecule with promising results is the synthetic pseudopeptide NucAnt N6L (N6L, Figure 5),[65] a pro-apoptotic compound able to exert antiproliferative activity and to inhibit tumor growth also *in vivo*, that has already completed phase I/II clinical trials for different solid tumors (2012-000939-42). Surface plasmon resonance assays with full-length NPM1 showed a strong interaction of the pseudopeptide with the

protein (K_D of 1 nM) and further studies revealed that N6L interacts with the N-terminus of NPM1 interfering with pentamer formation. In the same work, the authors established that this alteration by N6L results in the activation of p53 apoptotic pathway, leading to cell death. Interestingly, the cytotoxicity observed in *in vitro* models of AML with NPM1 wt is significantly higher than in *NPM1* mutation carriers, which exhibited striking resistance to treatment with the pseudopeptide.

In addition to small molecules, other types of compounds have been identified as NPM1 modulators. These include the aptamer 1A1 RNA,[66] which inhibits oligomerization by interacting with the IDR region adjacent to the N-terminal domain, and the peptide Rev37-47,[67,68] which interferes with NPM1 protein-protein interactions.

The results shown by the molecules described to date support the potential of direct modulation of NPM1 for the treatment of AML, with a particular focus on *NPM1*^{mut} AML. Hence, this approach merits further research to advance the cure of the disease. In this regard, previous work carried out in our group allowed us to identify **UCM-13369** as a novel NPM1 modulator from a microbiota-inspired library (see Section 1.4.).

1.4.Cancer-stem-cell phenotype-guided identification of the microbiota-inspired compound UCM-13369 as a novel NPM1 inhibitor with therapeutic potential for AML [69]

The microbiota is a dynamic system of more than 100 trillion micro-organism in our bodies. They form a complex ecosystem composed of a myriad of different species, such as protozoa, fungi, virus and bacteria, which can influence numerous physiological processes including digestion, metabolism, cognitive development and immune system.[70,71] It is estimated that they make up more than 22 million microbial genes, exceeding human ones. With these genes, collectively called microbiome, the microbiota can synthesize numerous enzymes with versatile capabilities to ferment a variety of compounds indigestible by human enzymes. As a result, a battery of metabolites is produced with a wide spectrum of bioactivities (modulation of energy metabolism, nutrition absorption, regulation of microbiota composition, etc.) that play an important role in health and disease.[72-74]

Under healthy conditions, these micro-organisms establish a symbiotic relationship with the host. However, when an imbalance of the microbiota occurs due to external changes, it can lead to deregulation of body functions and disease. So far, this dysbiosis has been related to neurodegenerative diseases, diabetes, heart pathologies, immune diseases or cancer.[75-80] For this reason, several therapies involving “healthy” microbiota metabolites have recently been implemented.[81,82] For instance, the administration of 6-formylindolo[3,2-b]carbazole (Ficz), a tryptophan metabolite, has proven therapeutic potential for different diseases, like endometritis or skin cancer.[83-85]

After considering the importance of microbiota metabolites in health and disease, our research group proposed that they may represent an unexplored chemical space of

small organic molecules in the search for initial hits towards the identification of novel drug candidates. To this end, the structures of identified small-molecule metabolites were analyzed and the repertoire of organocatalytic reactions was explored to generate a set of microbiota-inspired compounds that combine metabolite structural diversity with synthetic accessibility. Thus, based on privileged scaffolds (PrSc) found in the metabolites selected in Figure 6A and asymmetric amino catalytic reactions starting with a small group of aldehydes and nitroderivatives (Figure 6B), new chemotypes were synthesized containing a PrSC-based central core linked to the common PrSc *p*-methoxyphenyl as well as to a drug-like moiety that could favor good pharmacokinetic properties. In the designed molecules **I-XIII** (Figure 6C), the central cores are piperidin-2-one, piperidine, tetrahydro-1*H*-carbazole, chromane, and dihydropyrido[2,3-b]pyrazine. These systems are inspired on the metabolites 3-amino-2-piperidone, pipecolic acid, methyl 3-carbazolecarboxylate, equol, folic acid, trimethylpyrazine and γ-carboxyethylhydroxychroman (γ-CEHC) related to vitamin E, shown in Figure 6A. Organocatalysis was applied as a key methodology to obtain the new chemotypes with high structural complexity in a straightforward and stereocontrolled manner. Thus, the central cores were constructed in a single step and with high diastereoselectivities by reaction between an α,β-unsaturated aldehyde, a nitrocompound and/or a second aldehyde, promoted by diphenylprolinol trimethylsilyl ether catalyst (Figure 6C). Further transformation of the aldehyde and the nitro groups allowed to obtain compounds **I-XIII** that contain the drug-like moiety (cyclopropylmethyl)amine and an amino group.

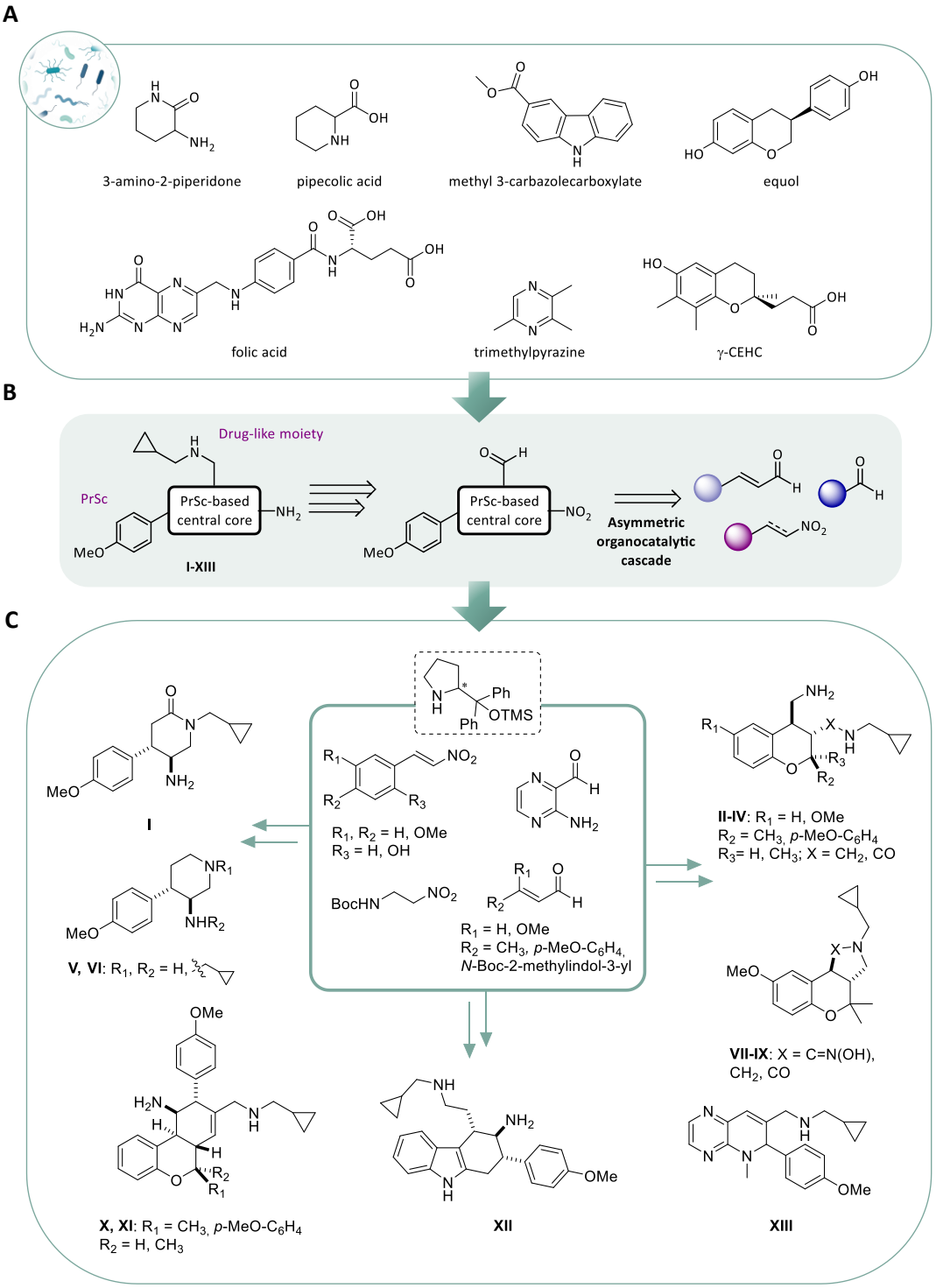

Figure 6. Design of the new chemotypes inspired on human microbiota metabolites. (A) Selected small-molecule metabolites produced by the microbiota. (B) Synthetic approach via asymmetric aminocatalysis to generate microbiota-inspired molecules **I-XIII**. (C) Overview of the synthetic strategy based on the reaction between an α,β-unsaturated aldehyde, a nitrocompound and/or a second aldehyde. PrSc: privileged scaffold. Untapered lines represent the relative stereochemistry.

Once the microbiota-inspired compounds were synthesized, their potential in cancer cellular models was explored with the ultimate goal to identify novel antitumor drug candidates. A phenotypic strategy was used, where the tested compounds are evaluated without prior knowledge of the target protein on which they act, so that new therapeutic targets can subsequently be identified.[86,87] Compounds **I-XIII** were screened in a cancer-stem-cell (CSC) phenotype assay that represents an advantageous opportunity, since existing therapies against these cells remain deficient, as most of them are directed to target biomarkers that are expressed not only by CSC, triggering unfortunate effects on cancer patients.[88-90] Notably, elimination of CSC in leukemia remains a major challenge, as their ineffective eradication is a primary contributing factor to relapse following remission.[91]

Hence, the cytotoxic effect of the new compounds in breast (MCF-7) and colon (HCT-116) tumor cell lines was determined using MTT assays. The formation of MCF-7-derived mamospheres and HCT-116-derived colonospheres in the presence of a non-cytotoxic concentration of the compounds was then assessed using bright field microscopy. The compound **UCM-13369**[92] (Figure 7A) was able to completely inhibit the formation of tumorspheres, a characteristic growth in CSC, without affecting the viability of differentiated tumor cells. In addition, the cytotoxicity of the compound was evaluated against IMR90 fibroblasts as control normal cells. These results showed that **UCM-13369** induced low levels of cytotoxicity in tumor cells (96% and 70% cell viability at 5 µM), complete inhibition of tumorsphere formation and no toxicity in fibroblasts (94% cell viability at 5 µM) (Figure 7B).

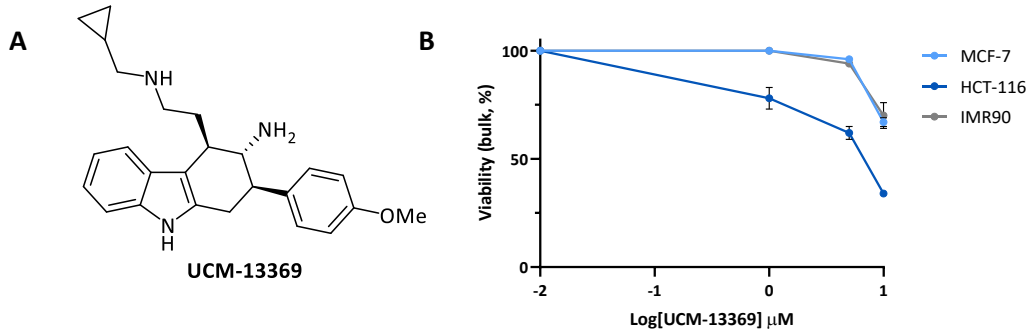

Figure 7. (A) Structure of compound **UCM-13369**. (B) Concentration-response curve of **UCM-13369** in MCF-7, HCT-116 and IMR90 cells.

With the aim to decipher the molecular targets of **UCM-13369**, proteomic experiments were carried out. Considering that AML is one of the most paradigmatic diseases with critical involvement of CSC and that among the AML stem population, $CD34^+/CD38^-$ are the only ones capable of inducing leukemia *in vivo,* these cells were used to identify the target proteins of **UCM-13369**. Thus, 1D-nano LC ESI-MS/MS proteomic analysis was performed in $CD34^+$ cells before and after **UCM-13369** treatment. The results showed multiple differentially expressed proteins; only those that disappeared

completely after treatment with the compound and whose concentration could be quantified in untreated samples were considered. According to this profile, 340 proteins, including targets related with stemness and cancer, were identified (Figure 8A). Among them, NPM1 especially attracted our attention, for its AML relevance mentioned in the previous sections. Western blot (WB) revealed reduced levels of NPM1 upon treatment with **UCM-13369** in MOLM13 cells expressing NPM1 wt (Figure 8B), which validated the proteomic results indicating NPM1 as a target protein of the compound.

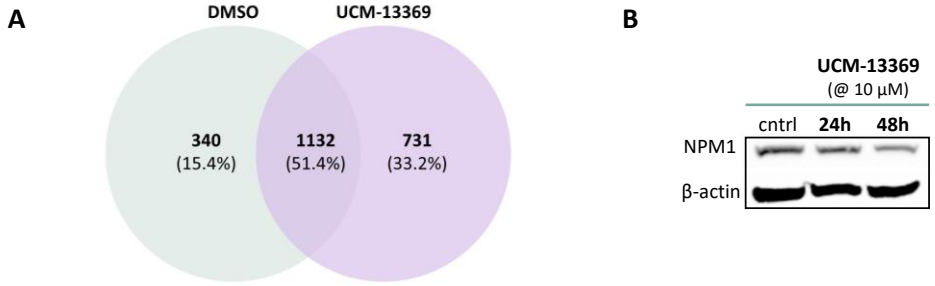

Figure 8. NPM1 protein is a molecular target of **UCM-13369**. (A) Venn diagram (Venny 2.1) of proteomic analysis of $CD34^+$ cells with and without **UCM-13369** treatment. (B) WB showed down-expression of NPM1 with **UCM-13369** treatment (10 µM) in MOLM13 cells at 24 and 48 h. Densitometry values: reduction of 5% and 44%, respectively.

To support that the inhibitory capacity of **UCM-13369** observed in CSC is mediated by NPM1, the compound was tested in MOLM13 and OCI-AML3 cell lines, as *in vitro* AML models bearing NPM1 wt and mutant (NPM1 C+) protein, respectively. The concentration-response curves obtained in the WST-1 assays (Figure 9A) indicated that the compound exhibits cytotoxicity against both cell lines in the micromolar range, showing higher efficacy in NPM1 C+ expressing cells (OCI-AML3: IC_{50} = 7.26 µM, MOLM13: IC_{50} = 10.89 µM, Figure 9A).

Considering the inhibitory capacity that **UCM-13369** showed in AML cell lines, the therapeutic potential was assessed in primary cells from AML patients. Healthy donors and AML patients were subjected to a surgical procedure to extract bone marrow from their rear pelvic bone and whole mononuclear cells were isolated through Ficoll centrifugation. Two *ex vivo* models were used from AML patients and healthy donors: $CD34^+$ liquid hematopoietic stem cell (HSC) culture as a short-term model and colony-forming unit-erythroid (CFU-E) as a mid-term model. **UCM-13369** induced decrease viability in AML patient cells, while exhibiting lower cytotoxicity in healthy donor cells (HSC: IC_{50} of 1.88 µM and 6.40 µM, Figure 9B; CFU-E: IC_{50} of 0.30 µM and 1.73 µM, Figure 9C; values for AML patients and healthy donors, respectively), providing a therapeutic window opportunity for the compound. Moreover, the compound demonstrated superior efficacy in AML patients harboring the *NPM1* mutation (IC_{50} = 1.73 µM) than in those lacking it (IC_{50} = 3.77 µM) (Figure 9D).

Additionally, flow cytometry experiments showed that the inhibition of NPM1 by **UCM-13369** correlates with the increase in apoptosis observed in treated primary CD34$^+$ cells upon staining with Annexin V (Figure 9E).

Together, our results confirm that CSC death induced by NPM1 inhibition represents a promising therapeutic opportunity for targeted treatment of *NPM1*^{mut} AML, a high-mortality disease.

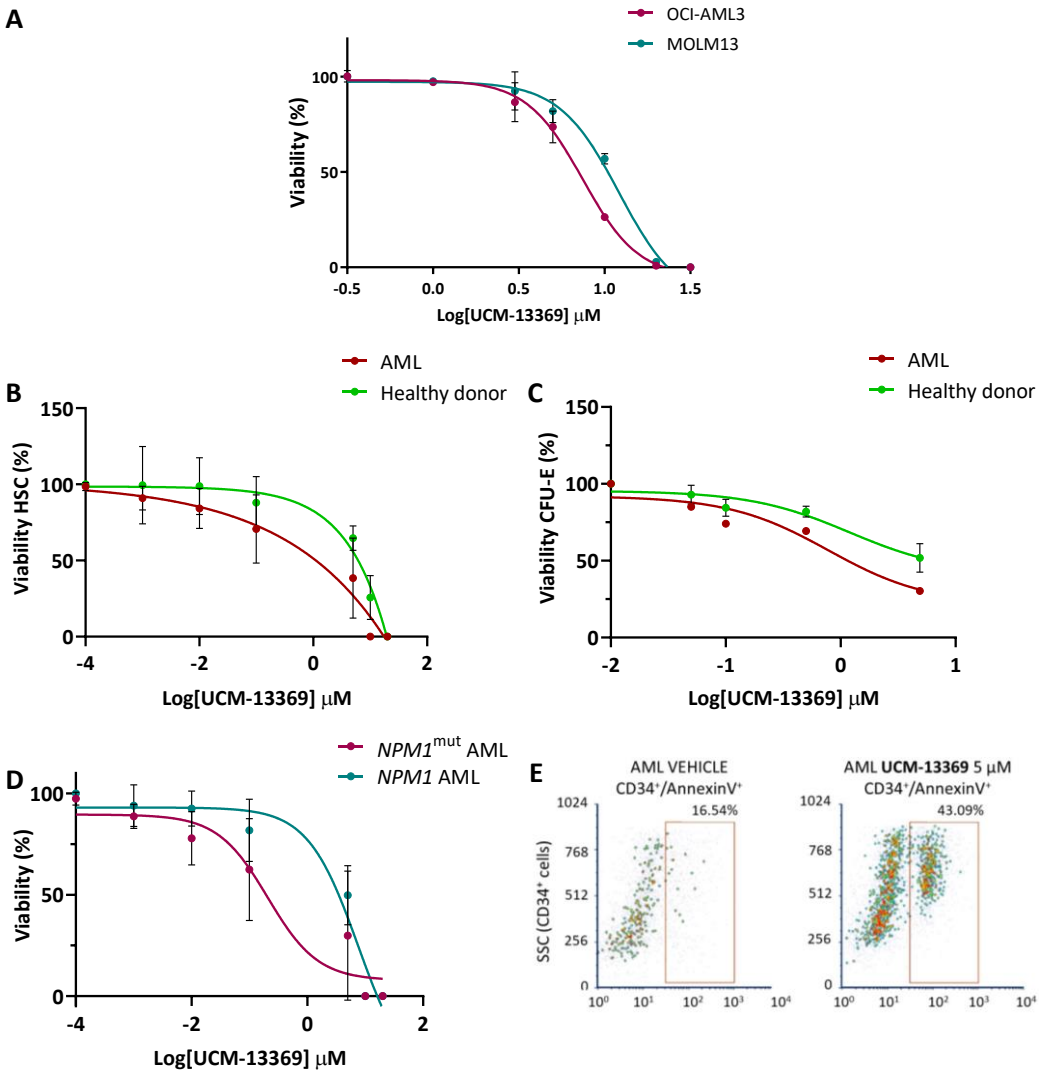

Figure 9. **UCM-13369** has efficacy against AML cell lines and AML patient cells. (A) Concentration-response curves of **UCM-13369** in AML cell lines MOLM13 (NPM1 wt) and OCI-AML3 (NPM1 C+). (B) Concentration-response curves of **UCM-13369** in short-term cultures of primary HSCs from bone marrow mononuclear fraction from healthy donors and AML patients. (C) Concentration-response curves of **UCM-13369** in colony formation unit (CFU) assays performed with primary HSCs bone marrow mononuclear fraction from healthy donors and AML patients. (D) Concentration-response curves of primary HSCs with samples from AML patients with NPM1 wt vs. NPM1 C+. (E) Dot plot of a representative sample from flow cytometry analysis using CD34-PE/AnnexinV-FITC staining of short-term cultures of primary HSCs from AML patients performed with primary HSCs from bone marrow mononuclear fraction with and without treatment.

OBJECTIVES

2. OBJECTIVES

NPM1 stands out as a particularly relevant protein in AML, a hematological disease with a high mortality rate. However, the number of small molecules described that interact directly with NPM1 is scarce and there are no NPM1 modulators currently used in clinical practice. The promising results previously obtained in our research group for the novel microbiota-inspired small molecule **UCM-13369** support the therapeutic potential of the new synthetic NPM1 inhibitor.

In this work, we aim to advance a drug candidate as a novel NPM1-targeted therapy for AML, which is critical for the future of patients, to improve their dramatically low survival rate. Toward this end, we will continue preclinical studies of **UCM-13369**, including extensive pharmacological characterization and *in vivo* efficacy assessment. If unsuccessful, we will undertake further optimization to develop new NPM1 modulators with the ultimate goal of identifying a drug candidate for AML treatment.

RESULTS AND DISCUSSION

3. RESULTS AND DISCUSSION

3.1.Characterization of UCM-13369 as a direct NPM1 modulator

Once **UCM-13369** (Figure 10) was identified as a modulator of NPM1 by differential proteomics and WB and having demonstrated its therapeutic potential in an *ex vivo* AML model, we considered it necessary to carry out an extensive pharmacological characterization of the compound. Specifically, it was important to define whether the observed effects were the result of a direct interaction between the compound and the NPM1 protein, or the effects of an alteration in the protein signaling pathway.

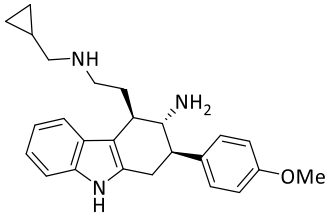

UCM-13369

Figure 10. Compound **UCM-13369** previously identified as a modulator of NPM1.

3.1.1.Study of the binding interaction

To further support NPM1 as a molecular target of **UCM-13369**, our first approach was to design a fluorescent probe that would allow us to visualize by confocal microscopy the intracellular colocalization of the compound and the protein. Thus, we synthesized probe **UCM-13369-SulfoCy5** (**1**, Figure 11), containing the fluorophore sulfocyanine-5 (SulfoCy5). This water-soluble fluorescent dye is well suited for biological assays due to its high photostability and strong emission around 670-690 nm, which minimizes the background autofluorescence of the biological matrix.

Probe **1** was obtained from compound **2**, a **UCM-13369** derivative, in which the cyclopropyl group was replaced by an alkyne to perform a click chemistry reaction with the fluorophore SulfoCy5 (Figure 11, see Section 5.1.3. for details).

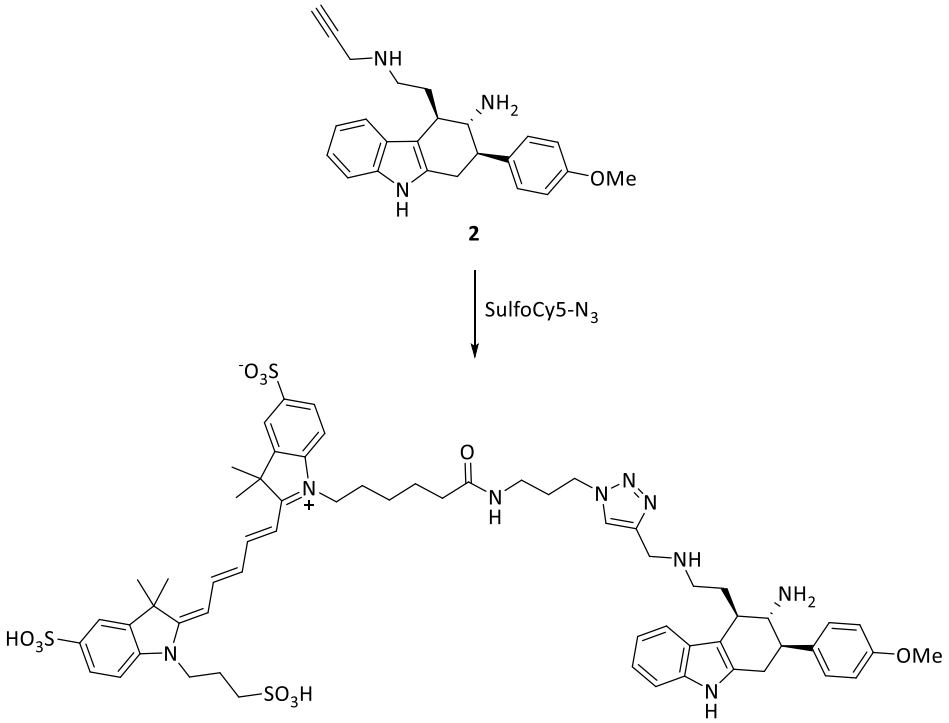

Figure 11. Fluorescent probe **UCM-13369-SulfoCy5** (**1**) used for confocal microscopy studies.

Synthesized probe **1** was used in confocal microscopy studies supervised by Dr. Miguel Gallardo at the Centro Nacional de Investigaciones Oncológicas (CNIO, Madrid). OCI-AML3 cells were treated with the probe, emitting in red, and incubated with Alexa-Fluor-488-conjugated NPM1 primary antibody, in green (Figure 12). The visualization of their overlap indicated colocalization of the compound with the protein.

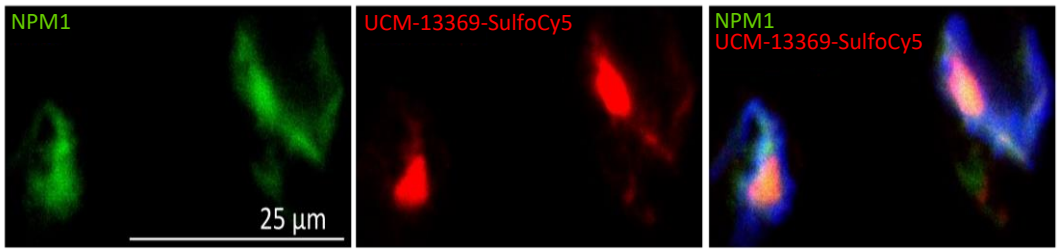

Figure 12. Confocal microscopy images with staining of NPM1 (Alexa-Fluor-488, green), **UCM-13369-SulfoCy5** (red) and nuclei (DAPI, blue) in OCI-AML3 cells.

To confirm a direct interaction between **UCM-13369** and NPM1 and to shed light on the binding domain of the protein, isothermal titration calorimetry (ITC) assays were performed, in collaboration with Prof. Irene Díaz-Moreno at the Centro de Investigaciones Científicas de la Cartuja (cicCartuja, Sevilla). For this purpose, pure protein samples of the pentameric N-terminal domain of NPM1 (1-130 amino acids) and the C-terminal domains of NPM1 wt and mutant NPM1 C+ were used. The experiments (Figure 13) revealed that

the interaction between NPM1 and **UCM-13369** occurs mainly through the C-terminus of the protein, showing the N-terminus a much lower binding affinity ($K_{D\ NPM1\ N\text{-}term}$ ca. 100 µM, $K_{D\ NPM1\ wt\ C\text{-}term}$ = 37 µM; Table 3). Importantly, the C-terminal domain of NPM1 C+ exhibited a two-fold higher affinity than the wt terminus ($K_{D\ NPM1\ C+}$ = 15 µM vs. $K_{D\ NPM1\ wt}$ = 37 µM; Table 3), which is in agreement with the activity results obtained for **UCM-13369** in OCI-AML3 (NPM1 C+) and MOLM13 (NPM1 wt) cell lines (OCI-AML3: IC_{50} = 7.26 µM, MOLM13: IC_{50} = 10.89 µM, respectively; Figure 9A). Additionally, the assays showed a binding stoichiometry approximately equal to 1 (n = 1.3, Table 3), indicating that one molecule of the compound interacts with one protein monomer, also in the case of the N-terminal domain, that was studied in its pentameric form (n = 7.7, Table 3). Altogether, ITC data suggest that the new NPM1 inhibitor **UCM-13369** binds specifically to the C-terminus of the protein.

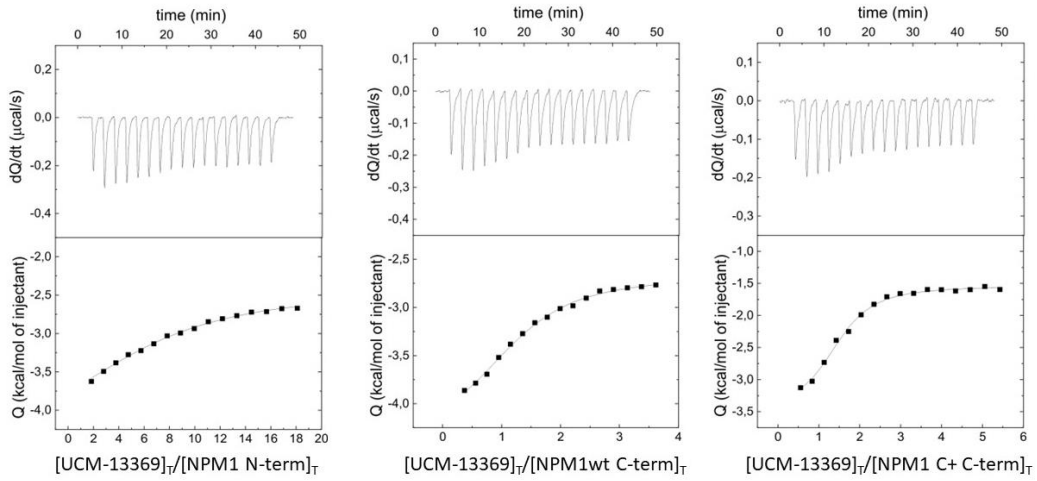

Figure 13. ITC thermograms and binding isotherms of the interaction of **UCM-13369** with the N-terminus of NPM1 (NPM1 N-term), the C-terminus of NPM1 wt (NPM1 wt C-term) and the C-terminus of NPM1 C+ (NPM1 C+ C-term).

Table 3. ITC-derived thermodynamic parameters of **UCM-13369**-NPM1 interaction: Gibbs free energy (Δ*G*), enthalpy (Δ*H*), entropic term (-TΔ*S*), equilibrium dissociation constant (K_D), and binding stoichiometry (n).

Protein variant	K_D (µM)	Δ*G* (kcal·mol^{-1})	Δ*H* (kcal·mol^{-1})	-TΔ*S* (kcal·mol^{-1})	n
NPM1 N-term	100	-5.4	-2.2	-3.2	7.7
NPM1 wt C-term	37	-6.0	-1.8	-4.2	1.3
NPM1 C+ C-term	15	-6.6	-2.0	-4.6	1.3

Errors: 0.1-0.2 kcal·mol^{-1} for ΔG, 0.3-0.5 kcal·mol^{-1} for ΔH and -TΔS, 0.2 for n, 10-20% for K_D. Protein concentration of the NPM1 N-terminus construct is referred to the pentamer, while those of the C-terminus correspond to the monomer.

Once the NPM1 binding domain for **UCM-13369** was identified, *ab initio* docking studies were performed using HADDOCK software (in collaboration with Prof. Irene Díaz-Moreno) to identify possible binding sites. The structure corresponding to the putative C-terminus of the wt protein characterized by NMR was retrieved from the PDB (2LLH). The refined docking yielded ten possible binding sites (clusters 1-10, Figure 14) through the surface of the C-terminal domain of the protein, suggesting that **UCM-13369** explores this surface stochastically. Among them, cluster 3 (shown in inset iv, Figure 14) exhibited the lowest desolvation energy and harbored the second largest buried surface area of all docking clusters analyzed. Notably, this cluster matched with the previously reported binding site of the small-molecule NPM1 ligands C1 and C3 (see Section 1.3.).[64]

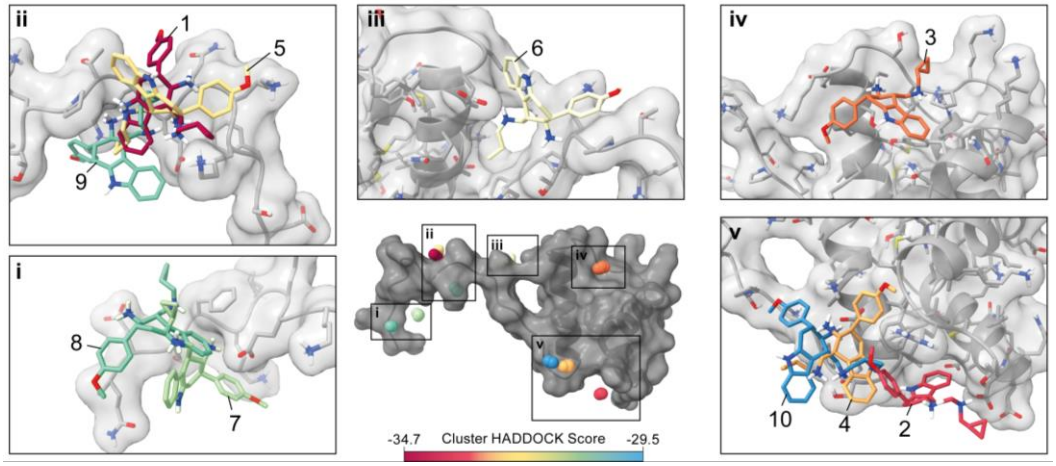

Figure 14. Visualization of **UCM-13369** binding interfaces to NPM1 wt C-terminal domain. The centroids of **UCM-13369** in the four lowest energy structures of each of the ten clusters are plotted as balls colored according to the HADDOCK score, as indicated in the color legend. The structure of **UCM-13369** of the top-ranked structure of each cluster (1-10) is represented in the insets i-v.

Additionally, we carried out saturation transfer difference nuclear magnetic resonance (STD-NMR) experiments supervised by Prof. Angeles Canales at Universidad Complutense de Madrid (UCM), to help elucidate the epitope of **UCM-13369**. Two spectra were acquired: off-resonance, used as reference; and on-resonance, where the interaction is recorded (Figure 15). The off-resonance spectrum was registered setting the irradiation frequency at a value far from any ligand or protein signal, whereas the on-resonance spectrum was obtained by selectively irradiating with a radiofrequency pulse affecting only the protein. According to the Nuclear Overhauser Effect (NOE), saturation is transferred from the protein to the ligand through intermolecular interactions, which results in a decrease in the signal of those protons in the ligand interacting with the protein. The decrease in the signal is directly proportional to the degree of interaction and can be quantified by subtracting the on-resonance spectrum from the off-resonance one, resulting in the STD spectrum. Hence, STD signals show the part of the molecule most buried in the protein.

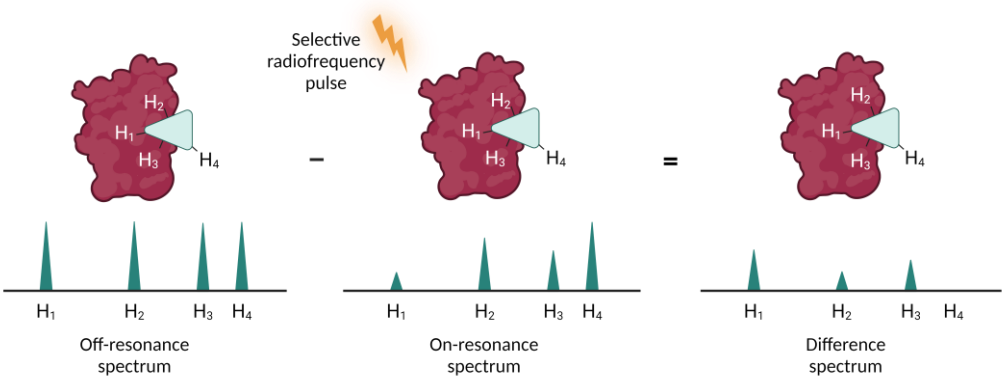

Figure 15. Schematic representation of an STD experiment. Signals in the difference spectrum indicate an interaction between the protons of the small molecule and the protein.

The STD-NMR experiment of **UCM-13369** was acquired using commercially available full-length NPM1 wt in the presence of a ten-fold excess of the compound relative to the protein (300 vs. 30 µM). As shown in Figure 16, clear STD signals were detected for **UCM-13369**, pointing out that the protein recognizes the compound. The STD spectrum displays signals that belong to two aromatic rings of the molecule, indicating that these systems are involved in the recognition. The highest values correspond to the protons of the aromatic ring of the tetrahydrocarbazole scaffold (H_5-H_8, Figure 16). Interestingly, these results are in agreement with the docking prediction since in the lower energy structures, corresponding to clusters 1-3 (Figure 14), the aromatic system of the tetrahydrocarbazole core is buried on the surface of NPM1 C-terminal domain.

Following structural studies, future work should aim to unravel the interaction of **UCM-13369** with the disordered C-terminal domain of NPM1 C+ in order to explain the higher binding that the compound exhibits towards it.

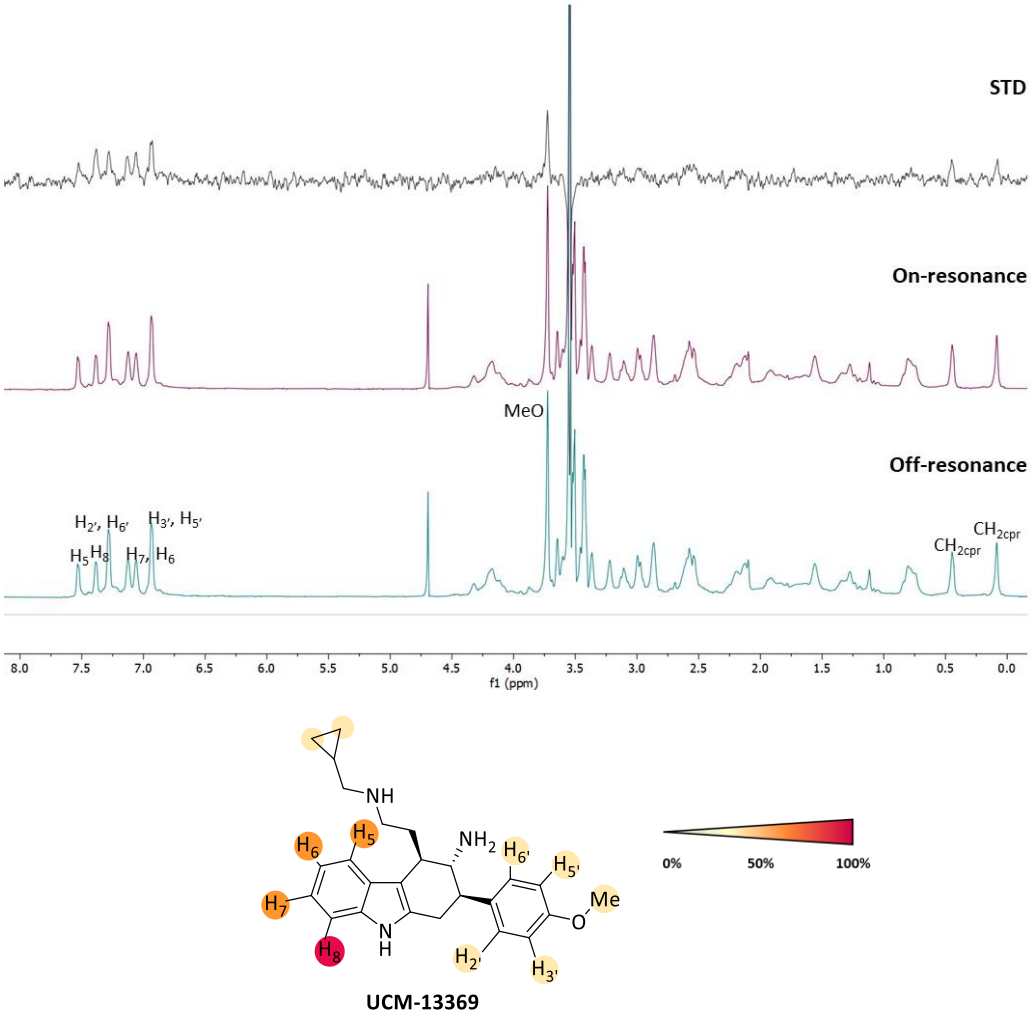

Figure 16. STD (black), on-resonance (magenta) and off-resonance (cyan) NMR spectra of **UCM-13369** in the presence of NPM1 wt protein. The intensity of the interaction of the protons is indicated by the color gradient.

3.1.2.Unraveling the molecular mechanism

For a deeper understanding of the effect of **UCM-13369** in AML cells, we studied the impact of the compound in the genes and the expression levels of NPM1 wt and NPM1 C+ pathway components, such as the positive regulation of oncoprotein c-Myc and the negative regulation of tumor suppressor FBXW7. These experiments were carried out under the supervision of Dr. Miguel Gallardo (CNIO). Thus, OCI-AML3 cells were incubated with the compound (10 µM) for 24 and 48 h (DMSO-treated cells as controls), then genes and protein levels were assessed by quantitative polymerase chain reaction (qPCR) and WB, respectively, revealing reduced levels for NPM1 and c-Myc, while FBXW7 was found to be upregulated in both cell lines (Figure 17).

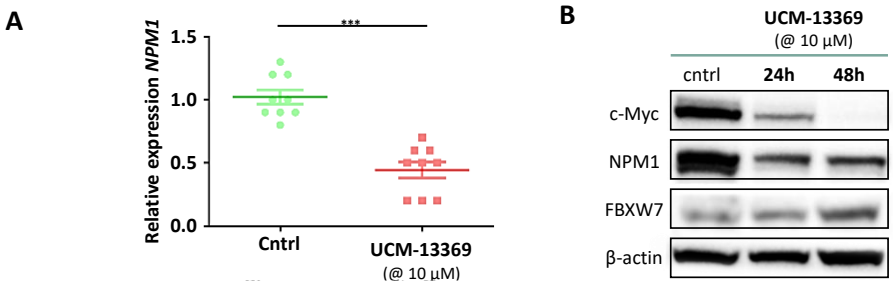

Figure 17. (A) Dot plot showing decreased *NPM1* expression with **UCM-13369** treatment (10 µM) in OCI-AML3 cells. (B) WB showing decreased NPM1 and c-Myc expression and increased FBXW7 expression with **UCM-13369** treatment (10 µM) in OCI-AML3 cells at 24 and 48 h. Densitometry values for NPM1: reduction of 50% and 70%, respectively.

To further elucidate the mechanism of action of **UCM-13369**, we studied the influence of the compound on the subcellular location of the protein by confocal microscopy, using AlexaFluor-647-conjugated NPM1 primary antibody emitting in red and DAPI staining for nuclei. As mentioned, OCI-AML3 cells are characterized by the primary location of NPM1 C+ in the cytoplasm, whereas in MOLM3 cells NPM1 wt is mainly located in the nucleus and nucleolus (Figure 18A). After incubation of OCI-AML3 cell lines with **UCM-13369** (10 µM), we visualized that NPM1, in red, disappeared from the cytoplasm (Figure 18A). Hence, the compound was able to restore the nucleolar location phenotype of the protein, similar to the phenotype observed in MOLM13 control cells. The scatter dot plots in Figure 18B show the nucleus/cytoplasm distribution of the protein in MOLM13 and treated and untreated OCI-AML3 cells. Importantly, the new NPM1 inhibitor was able to reverse the aberrant location of the protein, which is characteristic of the mutation and critical for the maintenance of the AML disorder.

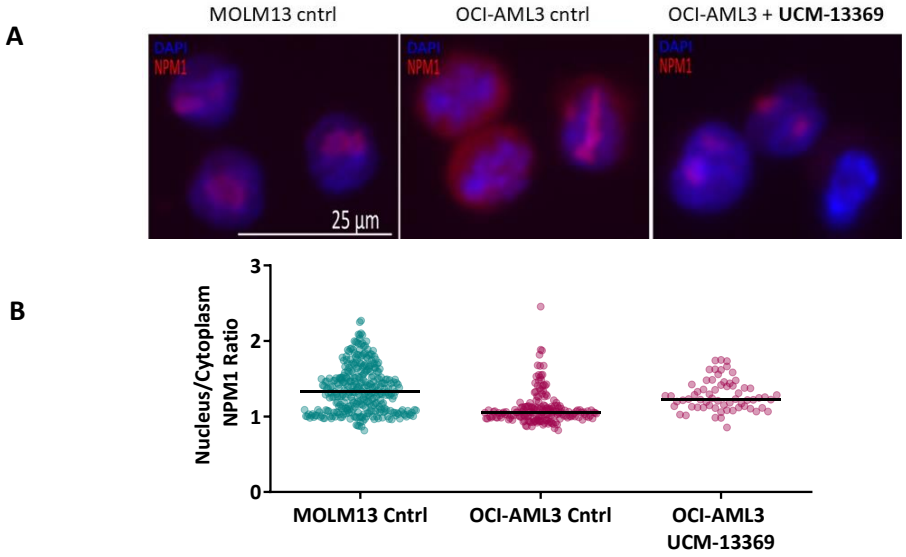

Figure 18. (A) Confocal microscopy images with NPM1 (Alexa-Fluor-647, red) and nuclei (DAPI, blue) staining in MOLM13, OCI-AML3, and **UCM-13369**-treated OCI-AML3 cells (10 µM). (B) Scatter

dot plot of NPM1 nucleus/cytoplasm ratio in MOLM13, OCI-AML3, and **UCM-13369**-treated OCI-AML3 cells.

3.1.3.Efficacy in an AML animal model

Based on the encouraging results obtained with **UCM-13369** in AML patient cells (see Section 1.4.), we decided to further evaluate its therapeutic potential *in vivo*. The efficacy was tested in immunodeficient mice injected with OCI-AML3-ffLuc-GFP cells as an *NPM1*^{mut} AML animal model, in collaboration with Dr. Gallardo. As shown in Figure 19A, the **UCM-13369**-treated group (50 mg/kg) showed a reduction of tumor infiltration compared to untreated group at end point, sustaining the efficacy of the compound against malignant cells. However, this effect did not result in an increase in survival, as no difference was observed between treated and untreated animals (Figure 19B). Analysis of the mice bone marrow using hematoxylin-eosin (H&E) staining revealed less tumor cell infiltration in treated mice, further supporting the efficacy of the compound for the treatment of AML (Figure 19C). Although caspase-3 pathology analysis of treated mice revealed the absence of toxicity in bone marrow and liver, some caspase-3 cleavage was observed in the kidney, pointing to some toxicity in this organ (Figure 19D).

Concentration−response viability assay in human renal proximal tubule epithelial cells (HRPTEpiC)[93,94] was performed and revealed toxicity (IC_{50} = 3.63 µM vs. OCI-AML3: IC_{50} = 7.26 µM, MOLM13: IC_{50} = 10.89 µM, Figure 19E), suggesting that renal toxicity could be one of the probable causes of lower-than-expected survival of treated AML animals.

The observed toxicity precludes further preclinical studies with the compound **UCM-13369**. However, the therapeutic evaluation both *ex vivo* in primary cells from AML patients and *in vivo* in the AML mouse model, together with the validation of NPM1 as a molecular target of the compound, support the potential of the tetrahydrocarbazole scaffold as worthy of further optimization. Therefore, we undertook a medicinal chemistry program around **UCM-13369** aimed at overcoming toxicity issues observed *in vivo* and developing an optimized NPM1 inhibitor, in terms of activity, toxicity and pharmacokinetic profile, as a drug candidate for the treatment of *NPM1* AML.

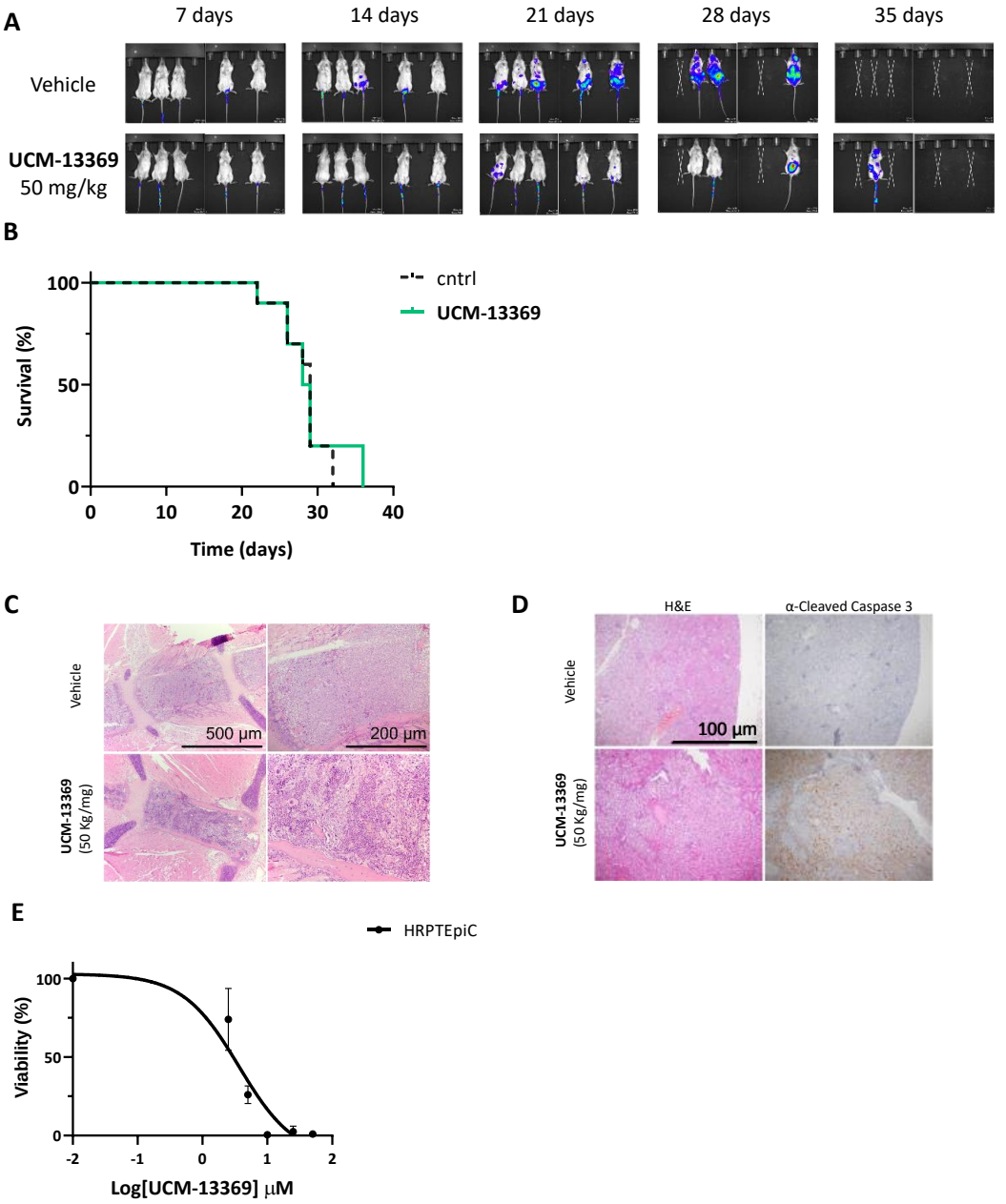

Figure 19. **UCM-13369** shows efficacy against AML cells *in vivo*. (A) Bioluminescence images acquired using an *in vivo* imaging system (IVIS) of NSG mice after injection of OCI-AML3 cell line with and without **UCM-13369** treatment (50 mg/kg). (B) Kaplan-Meir survival curve showed no significant differences between NSG mice injected with OCI-AML3 cells, with and without **UCM-13369** treatment (50 mg/kg). (C) Microscopy analysis of the OCI-AML3 infiltration by H&E staining slides of bone marrow samples from NSG mice with paired time points after engraftment with and without **UCM-13369** treatment (50 mg/kg). (D) IHC analysis of apoptotic cells in a representative kidney sample from OCI-AML3 xenograft mice treated with DMSO (vehicle, top) vs. **UCM-13369** treated mice (50 mg/kg, bottom): H&E (left) and cleaved caspase-3 (right). (E) Concentration-response curve of **UCM-13369** in human renal proximal tubule epithelial cells (HRPTEpiC) showed toxicity in kidney cells.

3.2.Medicinal chemistry program: synthesis and biological evaluation of structural analogues of UCM-13369

This section has been suppressed in this version due to confidentiality.

3.3.Pharmacological characterization *in vitro* of selected compounds

This section has been suppressed in this version due to confidentiality.

3.4.Therapeutic potential of candidates UCM-19282 and UCM-19286

This section has been suppressed in this version due to confidentiality.

CONCLUSIONS

4. CONCLUSIONS

This section has been suppressed in this version due to confidentiality.

.

EXPERIMENTAL SECTION

5. EXPERIMENTAL SECTION

This section has been suppressed in this version due to confidentiality.

REFERENCES

6. REFERENCES

(1) Döhner, H.; Weisdorf, D. J.; Bloomfield, C. D. Acute myeloid leukemia. *N. Engl. J. Med.* **2015**, *373*, 1136-1152.

(2) Makkar, H.; Majhi, R. K.; Goel, H.; Gupta, A. K.; Chopra, A.; Tanwar, P.; Seth, R. Acute myeloid leukemia: novel mutations and their clinical implications. *Am. J. Blood Res.* **2023**, *13*, 12-27.

(3) Arber, D. A.; Orazi, A.; Hasserjian, R.; Thiele, J.; Borowitz, M. J.; Le Beau, M. M.; Bloomfield, C. D.; Cazzola, M.; Vardiman, J. W. The 2016 revision to the World Health Organization classification of myeloid neoplasms and acute leukemia. *Blood* **2016**, *127*, 2391-2405.

(4) Swerdlow, S. H.; Campo, E.; Harris, N. L.; Jaffe, E. S.; Pileri, S. A.; Stein, H.; Thiele, J.; Vardiman, J. W. *WHO classification of tumours of haematopoietic and lymphoid tissues*; International agency for research on cancer Lyon, France, 2008.

(5) Arber, D. A.; Orazi, A.; Hasserjian, R. P.; Borowitz, M. J.; Calvo, K. R.; Kvasnicka, H.-M.; Wang, S. A.; Bagg, A.; Barbui, T.; Branford, S.; Bueso-Ramos, C. E.; Cortes, J. E.; Dal Cin, P.; DiNardo, C. D.; Dombret, H.; Duncavage, E. J.; Ebert, B. L.; Estey, E. H.; Facchetti, F.; Foucar, K.; Gangat, N.; Gianelli, U.; Godley, L. A.; Gökbuget, N.; Gotlib, J.; Hellström-Lindberg, E.; Hobbs, G. S.; Hoffman, R.; Jabbour, E. J.; Kiladjian, J.-J.; Larson, R. A.; Le Beau, M. M.; Loh, M. L.-C.; Löwenberg, B.; Macintyre, E.; Malcovati, L.; Mullighan, C. G.; Niemeyer, C.; Odenike, O. M.; Ogawa, S.; Orfao, A.; Papaemmanuil, E.; Passamonti, F.; Porkka, K.; Pui, C.-H.; Radich, J. P.; Reiter, A.; Rozman, M.; Rudelius, M.; Savona, M. R.; Schiffer, C. A.; Schmitt-Graeff, A.; Shimamura, A.; Sierra, J.; Stock, W. A.; Stone, R. M.; Tallman, M. S.; Thiele, J.; Tien, H.-F.; Tzankov, A.; Vannucchi, A. M.; Vyas, P.; Wei, A. H.; Weinberg, O. K.; Wierzbowska, A.; Cazzola, M.; Döhner, H.; Tefferi, A. International consensus classification of myeloid neoplasms and acute leukemias: integrating morphologic, clinical, and genomic data. *Blood* **2022**, *140*, 1200-1228.

(6) Martelli, M. P.; Pettirossi, V.; Thiede, C.; Bonifacio, E.; Mezzasoma, F.; Cecchini, D.; Pacini, R.; Tabarrini, A.; Ciurnelli, R.; Gionfriddo, I.; Manes, N.; Rossi, R.; Giunchi, L.; Oelschlagel, U.; Brunetti, L.; Gemei, M.; Delia, M.; Specchia, G.; Liso, A.; Di Ianni, M.; Di Raimondo, F.; Falzetti, F.; Del Vecchio, L.; Martelli, M. F.; Falini, B. CD34+ cells from AML with mutated NPM1 harbor cytoplasmic mutated nucleophosmin and generate leukemia in immunocompromised mice. *Blood* **2010**, *116*, 3907-3922.

(7) Short, N. J.; Konopleva, M.; Kadia, T. M.; Borthakur, G.; Ravandi, F.; DiNardo, C. D.; Daver, N. Advances in the treatment of acute myeloid leukemia: new drugs and new challenges. *Cancer Discov.* **2020**, *10*, 506-525.

(8) Sharma, N.; Liesveld, J. L. NPM 1 mutations in AML—The landscape in 2023. *Cancers* **2023**, *15*, 1177.

(9) Bertoli, S.; Tavitian, S.; Bérard, E.; Mansat-De Mas, V.; Largeaud, L.; Gadaud, N.; Rieu, J.-B.; Vergez, F.; Luquet, I.; Huguet, F. More than ten percent of relapses occur after five years in AML patients with NPM1 mutation. *Leuk. Lymphoma* **2020**, *61*, 1226-1229.

(10) Box, J. K.; Paquet, N.; Adams, M. N.; Boucher, D.; Bolderson, E.; O'Byrne, K. J.; Richard, D. J. Nucleophosmin: from structure and function to disease development. *BMC Mol. Biol.* **2016**, *17*, 19.

(11) Lindström, M. S. NPM1/B23: a multifunctional chaperone in ribosome biogenesis and chromatin remodeling. *Biochem. Res. Int.* **2011**, *2011*, 1-16.

(12) Saluri, M.; Leppert, A.; Gese, G. V.; Sahin, C.; Lama, D.; Kaldmae, M.; Chen, G.; Elofsson, A.; Allison, T. M.; Arsenian-Henriksson, M.; Johansson, J.; Lane, D. P.; Hallberg, B. M.; Landreh, M. A "grappling hook" interaction connects self-assembly and chaperone activity of Nucleophosmin 1. *PNAS Nexus* **2023**, *2*, 303.

(13) Lee, H. H.; Kim, H. S.; Kang, J. Y.; Lee, B. I.; Ha, J. Y.; Yoon, H. J.; Lim, S. O.; Jung, G.; Suh, S. W. Crystal structure of human nucleophosmin-core reveals plasticity of the pentamer–pentamer interface. *Proteins: Struct., Funct., Bioinf.* **2007**, *69*, 672-678.

(14) Mitrea, D. M.; Cika, J. A.; Stanley, C. B.; Nourse, A.; Onuchic, P. L.; Banerjee, P. R.; Phillips, A. H.; Park, C.-G.; Deniz, A. A.; Kriwacki, R. W. Self-interaction of NPM1 modulates multiple mechanisms of liquid–liquid phase separation. *Nat. Commun.* **2018**, *9*, 842.

(15) Hisaoka, M.; Nagata, K.; Okuwaki, M. Intrinsically disordered regions of nucleophosmin/B23 regulate its RNA binding activity through their inter- and intra-molecular association. *Nucleic Acids Res.* **2013**, *42*, 1180-1195.

(16) Gallo, A.; Sterzo, C. L.; Mori, M.; Di Matteo, A.; Bertini, I.; Banci, L.; Brunori, M.; Federici, L. Structure of nucleophosmin DNA-binding domain and analysis of its complex with a G-quadruplex sequence from the c-MYC promoter. *J. Biol. Chem.* **2012**, *287*, 26539-26548.

(17) Grummitt, C. G.; Townsley, F. M.; Johnson, C. M.; Warren, A. J.; Bycroft, M. Structural consequences of nucleophosmin mutations in acute myeloid leukemia. *J. Biol. Chem.* **2008**, *283*, 23326-23332.

(18) Rose, A. S.; Bradley, A. R.; Valasatava, Y.; Duarte, J. M.; Prlić, A.; Rose, P. W. NGL viewer: web-based molecular graphics for large complexes. *Bioinformatics* **2018**, *34*, 3755-3758.

(19) Hindley, A.; Catherwood, M. A.; McMullin, M. F.; Mills, K. I. Significance of NPM1 gene mutations in AML. *Int. J. Mol. Sci.* **2021**, *22*, 10040.

(20) Brodská, B.; Šašinková, M.; Kuželová, K. Nucleophosmin in leukemia: consequences of anchor loss. *Int. J. Biochem. Cell Biol.* **2019**, *111*, 52-62.

(21) Kunchala, P.; Kuravi, S.; Jensen, R.; McGuirk, J.; Balusu, R. When the good go bad: mutant NPM1 in acute myeloid leukemia. *Blood Rev.* **2018**, *32*, 167-183.

(22) Verhaak, R. G.; Goudswaard, C. S.; van Putten, W.; Bijl, M. A.; Sanders, M. A.; Hugens, W.; Uitterlinden, A. G.; Erpelinck, C. A.; Delwel, R.; Lowenberg, B.; Valk, P. J. Mutations in nucleophosmin (NPM1) in acute myeloid leukemia (AML): association with other gene abnormalities and previously established gene expression signatures and their favorable prognostic significance. *Blood* **2005**, *106*, 3747-3754.

(23) Federici, L.; Falini, B. Nucleophosmin mutations in acute myeloid leukemia: a tale of protein unfolding and mislocalization. *Protein Sci.* **2013**, *22*, 545-556.

(24) Grummitt, C. G.; Townsley, F. M.; Johnson, C. M.; Warren, A. J.; Bycroft, M. Structural consequences of nucleophosmin mutations in acute myeloid leukemia. *J. Biol. Chem.* **2008**, *283*, 23326-23332.

(25) Colombo, E.; Martinelli, P.; Zamponi, R.; Shing, D. C.; Bonetti, P.; Luzi, L.; Volorio, S.; Bernard, L.; Pruneri, G.; Alcalay, M. Delocalization and destabilization of the Arf tumor suppressor by the leukemia-associated NPM mutant. *Cancer Res.* **2006**, *66*, 3044-3050.

(26) Bonetti, P.; Davoli, T.; Sironi, C.; Amati, B.; Pelicci, P. G.; Colombo, E. Nucleophosmin and its AML-associated mutant regulate c-Myc turnover through Fbw7γ. *J. Cell Biol.* **2008**, *182*, 19-26.

(27) Falini, B.; Martelli, M. P.; Brunetti, L. Mutant NPM1: nuclear export and the mechanism of leukemogenesis. *Am. J. Hematol.* **2023**, *98*, 550-552.

(28) Brunetti, L.; Gundry, M. C.; Sorcini, D.; Guzman, A. G.; Huang, Y. H.; Ramabadran, R.; Gionfriddo, I.; Mezzasoma, F.; Milano, F.; Nabet, B.; Buckley, D. L.; Kornblau, S. M.; Lin, C. Y.; Sportoletti, P.; Martelli, M. P.; Falini, B.; Goodell, M. A. Mutant NPM1 maintains the leukemic state through HOX expression. *Cancer Cell* **2018**, *34*, 499-512.

(29) Heath, E. M.; Chan, S. M.; Minden, M. D.; Murphy, T.; Shlush, L. I.; Schimmer, A. D. Biological and clinical consequences of NPM1 mutations in AML. *Leukemia* **2017**, *31*, 798-807.

(30) Uckelmann, H. J.; Haarer, E. L.; Takeda, R.; Wong, E. M.; Hatton, C.; Marinaccio, C.; Perner, F.; Rajput, M.; Antonissen, N. J. C.; Wen, Y.; Yang, L.; Brunetti, L.; Chen, C. W.; Armstrong, S. A. Mutant NPM1 directly regulates oncogenic transcription in acute myeloid leukemia. *Cancer Discov.* **2023**, *13*, 746-765.

(31) Falini, B.; Brunetti, L.; Martelli, M. P. How I diagnose and treat NPM1-mutated AML. *Blood* **2021**, *137*, 589-599.

(32) Jimenez-Chillon, C.; Othman, J.; Taussig, D.; Jimenez-Vicente, C.; Martinez-Roca, A.; Tiong, I. S.; Jain, M.; Aries, J.; Cakmak, S.; Knapper, S.; Kristensen, D. T.; Murthy, V.; Galani, J. Z.; Kallmeyer, C.; Ngu, L.; Veale, D.; Bolam, S.; Orfali, N.; Parker, A.; Manson, C.; Parker, J.; Erblich, T.; Richardson, D.; Mokretar, K.; Potter, N.; Overgaard, U. M.; Roug, A. S.; Wei, A. H.; Esteve, J.; Jädersten, M.; Russell, N.; Dillon, R. Venetoclax-based low intensity therapy in molecular failure of NPM1-mutated AML. *Blood Adv.* **2024**, *8*, 343-352.

(33) Lai, C.; Doucette, K.; Norsworthy, K. Recent drug approvals for acute myeloid leukemia. *J. Hematol. Oncol.* **2019**, *12*, 100.

(34) Estey, E.; Karp, J. E.; Emadi, A.; Othus, M.; Gale, R. P. Recent drug approvals for newly diagnosed acute myeloid leukemia: gifts or a Trojan horse? *Leukemia* **2020**, *34*, 671-681.

(35) Ranieri, R.; Pianigiani, G.; Sciabolacci, S.; Perriello, V. M.; Marra, A.; Cardinali, V.; Pierangeli, S.; Milano, F.; Gionfriddo, I.; Brunetti, L.; Martelli, M. P.; Falini, B. Current status and future perspectives in targeted therapy of NPM1-mutated AML. *Leukemia* **2022**, *36*, 2351-2367.

(36) Wang, R.; Xu, P.; Chang, L. L.; Zhang, S. Z.; Zhu, H. H. Targeted therapy in NPM1-mutated AML: Knowns and unknowns. *Front. Oncol.* **2022**, *12*, 972606.

(37) Shi, Y.; Xue, Y.; Wang, C.; Yu, L. Nucleophosmin 1: from its pathogenic role to a tantalizing therapeutic target in acute myeloid leukemia. *Hematology* **2022**, *27*, 609-619.

(38) Hing, Z. A.; Fung, H. Y. J.; Ranganathan, P.; Mitchell, S.; El-Gamal, D.; Woyach, J. A.; Williams, K.; Goettl, V. M.; Smith, J.; Yu, X. Next-generation XPO1 inhibitor shows improved efficacy and in vivo tolerability in hematological malignancies. *Leukemia* **2016**, *30*, 2364-2372.

(39) Etchin, J.; Berezovskaya, A.; Conway, A. S.; Galinsky, I. A.; Stone, R. M.; Baloglu, E.; Senapedis, W.; Landesman, Y.; Kauffman, M.; Shacham, S. KPT-8602, a second-generation inhibitor of XPO1-mediated nuclear export, is well tolerated and highly active against AML blasts and leukemia-initiating cells. *Leukemia* **2017**, *31*, 143-150.

(40) Gionfriddo, I.; Brunetti, L.; Mezzasoma, F.; Milano, F.; Cardinali, V.; Ranieri, R.; Venanzi, A.; Pierangeli, S.; Vetro, C.; Spinozzi, G.; Dorillo, E.; Wu, H. C.; Berthier, C.; Ciurnelli, R.; Griffin, M. J.; Jennings, C. E.; Tiacci, E.; Sportoletti, P.; Falzetti, F.; de Thé, H.; Veal, G. J.; Martelli, M. P.; Falini, B. Dactinomycin induces complete remission associated with nucleolar stress response in relapsed/refractory NPM1-mutated AML. *Leukemia* **2021**, *35*, 2552-2562.

(41) Wu, H.-C.; Rérolle, D.; Berthier, C.; Hleihel, R.; Sakamoto, T.; Quentin, S.; Benhenda, S.; Morganti, C.; Wu, C.; Conte, L. Actinomycin D targets NPM1c-primed mitochondria to restore PML-driven senescence in AML therapy. *Cancer Discov.* **2021**, *11*, 3198-3213.

(42) Martelli, M. P.; Gionfriddo, I.; Mezzasoma, F.; Milano, F.; Pierangeli, S.; Mulas, F.; Pacini, R.; Tabarrini, A.; Pettirossi, V.; Rossi, R.; Vetro, C.; Brunetti, L.; Sportoletti, P.; Tiacci, E.; Di Raimondo, F.; Falini, B. Arsenic trioxide and all-trans retinoic acid target NPM1 mutant oncoprotein levels and induce apoptosis in NPM1-mutated AML cells. *Blood* **2015**, *125*, 3455-3465.

(43) Cierpicki, T.; Grembecka, J. Challenges and opportunities in targeting the menin–MLL interaction. *Future Med. Chem.* **2014**, *6*, 447-462.

(44) Fiskus, W.; Boettcher, S.; Daver, N.; Mill, C. P.; Sasaki, K.; Birdwell, C. E.; Davis, J. A.; Takahashi, K.; Kadia, T. M.; DiNardo, C. D. Effective Menin inhibitor-based combinations against AML with MLL rearrangement or NPM1 mutation (NPM1c). *Blood Cancer J.* **2022**, *12*, 5.

(45) Gundry, M. C.; Goodell, M. A.; Brunetti, L. It's all about MEis: menin-MLL inhibition eradicates NPM1-mutated and MLL-rearranged acute leukemias in mice. *Cancer Cell* **2020**, *37*, 267-269.

(46) Uckelmann, H. J.; Kim, S. M.; Wong, E. M.; Hatton, C.; Giovinazzo, H.; Gadrey, J. Y.; Krivtsov, A. V.; Rücker, F. G.; Döhner, K.; McGeehan, G. M. Therapeutic targeting of preleukemia cells in a mouse model of NPM1 mutant acute myeloid leukemia. *Science* **2020**, *367*, 586-590.

(47) Issa, G. C.; Aldoss, I.; DiPersio, J.; Cuglievan, B.; Stone, R.; Arellano, M.; Thirman, M. J.; Patel, M. R.; Dickens, D. S.; Shenoy, S.; Shukla, N.; Kantarjian, H.; Armstrong, S. A.; Perner, F.; Perry, J. A.; Rosen, G.; Bagley, R. G.; Meyers, M. L.; Ordentlich, P.; Gu, Y.; Kumar, V.; Smith, S.; McGeehan, G. M.; Stein, E. M. The menin inhibitor revumenib in KMT2A-rearranged or NPM1-mutant leukaemia. *Nature* **2023**, *615*, 920-924.

(48) Cela, I.; Di Matteo, A.; Federici, L. Nucleophosmin in its interaction with ligands. *Int. J. Mol. Sci.* **2020**, *21*, 4885.

(49) Di Matteo, A.; Franceschini, M.; Chiarella, S.; Rocchio, S.; Travaglini-Allocatelli, C.; Federici, L. Molecules that target nucleophosmin for cancer treatment: an update. *Oncotarget* **2016**, *7*, 44821.

(50) Florio, D.; Marasco, D. Could targeting NPM1c+ misfolding be a promising strategy for combating acute myeloid leukemia? *Int. J. Mol. Sci.* **2024**, *25*, 811.

(51) Mukherjee, H.; Chan, K. P.; Andresen, V.; Hanley, M. L.; Gjertsen, B. T.; Myers, A. G. Interactions of the natural product (+)-avrainvillamide with nucleophosmin and exportin-1. Mediate the cellular localization of nucleophosmin and its AML-associated mutants. *ACS Chem. Biol.* **2015**, *10*, 855-863.

(52) Wulff, J. E.; Siegrist, R.; Myers, A. G. The natural product avrainvillamide binds to the oncoprotein nucleophosmin. *J. Am. Chem. Soc.* **2007**, *129*, 14444-14451.

(53) Andresen, V.; Erikstein, B. S.; Mukherjee, H.; Sulen, A.; Popa, M.; Sørnes, S.; Reikvam, H.; Chan, K.-P.; Hovland, R.; McCormack, E. Anti-proliferative activity of the NPM1 interacting natural product avrainvillamide in acute myeloid leukemia. *Cell Death Dis.* **2016**, *7*, e2497-e2497.

(54) Yi, S.; Wen, L.; He, J.; Wang, Y.; Zhao, F.; Zhao, J.; Zhao, Z.; Cui, G.; Chen, Y. Deguelin, a selective silencer of the NPM1 mutant, potentiates apoptosis and induces differentiation in AML cells carrying the NPM1 mutation. *Ann. Hematol.* **2015**, *94*, 201-210.

(55) Chun, K.-H.; Kosmeder, J. W.; Sun, S.; Pezzuto, J. M.; Lotan, R.; Hong, W. K.; Lee, H.-Y. Effects of deguelin on the phosphatidylinositol 3-kinase/Akt pathway and apoptosis in premalignant human bronchial epithelial cells. *J. Natl. Cancer Inst.* **2003**, *95*, 291-302.

(56) Zhang, X.; Zhao, Z.; Yi, S.; Wen, L.; He, J.; Hu, J.; Ruan, J.; Fang, J.; Chen, Y. Deguelin induced differentiation of mutated NPM1 acute myeloid leukemia in vivo and in vitro. *Anti-Cancer Drugs* **2017**, *28*, 723-738.

(57) Qi, W.; Shakalya, K.; Stejskal, A.; Goldman, A.; Beeck, S.; Cooke, L.; Mahadevan, D. NSC348884, a nucleophosmin inhibitor disrupts oligomer formation and induces apoptosis in human cancer cells. *Oncogene* **2008**, *27*, 4210-4220.

(58) Balusu, R.; Fiskus, W.; Rao, R.; Chong, D. G.; Nalluri, S.; Mudunuru, U.; Ma, H.; Chen, L.; Venkannagari, S.; Ha, K.; Abhyankar, S.; Williams, C.; McGuirk, J.; Khoury, H. J.; Ustun, C.; Bhalla, K. N. Targeting levels or oligomerization of nucleophosmin 1 induces differentiation and loss of survival of human AML cells with mutant NPM1. *Blood* **2011**, *118*, 3096-3106.

(59) Šašinková, M.; Heřman, P.; Holoubek, A.; Strachotová, D.; Otevřelová, P.; Grebeňová, D.; Kuželová, K.; Brodská, B. NSC348884 cytotoxicity is not mediated by inhibition of nucleophosmin oligomerization. *Sci. Rep.* **2021**, *11*, 1084.

(60) Sekhar, K. R.; Reddy, Y. T.; Reddy, P. N.; Crooks, P. A.; Venkateswaran, A.; McDonald, W. H.; Geng, L.; Sasi, S.; Van Der Waal, R. P.; Roti, J. L. R. The novel chemical entity YTR107 inhibits recruitment of nucleophosmin to sites of DNA damage, suppressing repair of DNA double-strand breaks and enhancing radiosensitization. *Clin. Cancer Res.* **2011**, *17*, 6490-6499.

(61) Traver, G.; Sekhar, K. R.; Crooks, P. A.; Keeney, D. S.; Freeman, M. L. Targeting NPM1 in irradiated cells inhibits NPM1 binding to RAD51, RAD51 foci formation and radiosensitizes NSCLC. *Cancer Lett.* **2021**, *500*, 220-227.

(62) Penthala, N. R.; Crooks, P. A.; Freeman, M. L.; Sekhar, K. R. Development and validation of a novel assay to identify radiosensitizers that target nucleophosmin 1. *Bioorg. Med. Chem.* **2015**, *23*, 3681-3686.

(63) Penthala, N. R.; Ketkar, A.; Sekhar, K. R.; Freeman, M. L.; Eoff, R. L.; Balusu, R.; Crooks, P. A. 1-Benzyl-2-methyl-3-indolylmethylene barbituric acid derivatives: Anti-cancer agents that target nucleophosmin 1 (NPM1). *Bioorg. Med. Chem.* **2015**, *23*, 7226-7233.

(64) Urbaneja, M. A.; Skjaerven, L.; Aubi, O.; Underhaug, J.; Lopez, D. J.; Arregi, I.; Alonso-Marino, M.; Cuevas, A.; Rodriguez, J. A.; Martinez, A.; Banuelos, S. Conformational stabilization as a strategy to prevent nucleophosmin mislocalization in leukemia. *Sci. Rep.* **2017**, *7*, 13959.

(65) De Cola, A.; Franceschini, M.; Di Matteo, A.; Colotti, G.; Celani, R.; Clemente, E.; Ippoliti, R.; Cimini, A.; Dhez, A.; Vallée, B. N6L pseudopeptide interferes with nucleophosmin protein-protein interactions and sensitizes leukemic cells to chemotherapy. *Cancer Lett.* **2018**, *412*, 272-282.

(66) Jian, Y.; Gao, Z.; Sun, J.; Shen, Q.; Feng, F.; Jing, Y.; Yang, C. RNA aptamers interfering with nucleophosmin oligomerization induce apoptosis of cancer cells. *Oncogene* **2009**, *28*, 4201-4211.

(67) Fankhauser, C.; Izaurralde, E.; Adachi, Y.; Wingfield, P.; Laemmli, U. K. Specific complex of human immunodeficiency virus type 1 rev and nucleolar B23 proteins: dissociation by the Rev response element. *Mol. Cell. Biol.* **1991**, *11*, 2567–2575.

(68) Szebeni, A.; Herrera, J. E.; Olson, M. O. Interaction of nucleolar protein B23 with peptides related to nuclear localization signals and its modulation by phosphorylation. *Biochem.* **1995**, *34*, 8037-8042.

(69) Algar, S.; Vázquez-Villa, H.; Aguilar-Garrido, P.; Navarro-Aguadero, M. Á.; Velasco-Estévez, M. a.; Sánchez-Merino, A.; Arribas-Álvarez, I.; Paradela, A.; Giner-Arroyo, R. L.; Tamargo-Azpilicueta, J.; Díaz-Moreno, I.; Martínez-López, J.; Gallardo, M.; López-Rodríguez, M. L.; Benhamú, B. Cancer-stem-cell phenotype-guided discovery of a microbiota-inspired synthetic compound targeting NPM1 for leukemia. *JACS Au* **2024**, 1786–1800.

(70) McCarville, J. L.; Chen, G. Y.; Cuevas, V. D.; Troha, K.; Ayres, J. S. Microbiota metabolites in health and disease. *Annu. Rev. Immunol.* **2020**, *38*, 147-170.

(71) Aggarwal, N.; Kitano, S.; Puah, G. R. Y.; Kittelmann, S.; Hwang, I. Y.; Chang, M. W. Microbiome and human health: current understanding, engineering, and enabling technologies. *Chem. Rev.* **2022**, *123*, 31-72.

(72) Hou, K.; Wu, Z.-X.; Chen, X.-Y.; Wang, J.-Q.; Zhang, D.; Xiao, C.; Zhu, D.; Koya, J. B.; Wei, L.; Li, J. Microbiota in health and diseases. *Signal Transduct. Target Ther.* **2022**, *7*, 1-28.

(73) Yang, W.; Cong, Y. Gut microbiota-derived metabolites in the regulation of host immune responses and immune-related inflammatory diseases. *Cell. Mol. Immunol.* **2021**, *18*, 866-877.

(74) Rooks, M. G.; Garrett, W. S. Gut microbiota, metabolites and host immunity. *Nat. Rev. Immunol.* **2016**, *16*, 341-352.

(75) Chaudhari, S. N.; McCurry, M. D.; Devlin, A. S. Chains of evidence from correlations to causal molecules in microbiome-linked diseases. *Nat. Chem. Biol.* **2021**, *17*, 1046-1056.

(76) Sadrekarimi, H.; Gardanova, Z. R.; Bakhshesh, M.; Ebrahimzadeh, F.; Yaseri, A. F.; Thangavelu, L.; Hasanpoor, Z.; Zadeh, F. A.; Kahrizi, M. S. Emerging role of human microbiome in cancer development and response to therapy: special focus on intestinal microflora. *J. Transl. Med.* **2022**, *20*, 301.

(77) Wang, R.; Yang, X.; Liu, J.; Zhong, F.; Zhang, C.; Chen, Y.; Sun, T.; Ji, C.; Ma, D. Gut microbiota regulates acute myeloid leukaemia via alteration of intestinal barrier function mediated by butyrate. *Nat. Commun.* **2022**, *13*, 2522.

(78) Helmink, B. A.; Khan, M. W.; Hermann, A.; Gopalakrishnan, V.; Wargo, J. A. The microbiome, cancer, and cancer therapy. *Nat. Med.* **2019**, *25*, 377-388.

(79) Papadopoulos, P. D.; Tsigalou, C.; Valsamaki, P. N.; Konstantinidis, T. G.; Voidarou, C.; Bezirtzoglou, E. The emerging role of the gut microbiome in cardiovascular disease: Current knowledge and perspectives. *Biomedicines* **2022**, *10*, 948.

(80) Sasso, J. M.; Ammar, R. M.; Tenchov, R.; Lemmel, S.; Kelber, O.; Grieswelle, M.; Zhou, Q. A. Gut microbiome–brain alliance: a landscape view into mental and gastrointestinal health and disorders. *ACS Chem. Neurosci.* **2023**, *14*, 1717-1763.

(81) Saha, S.; Rajpal, D. K.; Brown, J. R. Human microbial metabolites as a source of new drugs. *Drug discovery today* **2016**, *21*, 692-698.

(82) Turroni, S.; Brigidi, P.; Cavalli, A.; Candela, M. Microbiota–host transgenomic metabolism, bioactive molecules from the inside: Miniperspective. *J. Med. Chem.* **2018**, *61*, 47-61.

(83) Rannug, A. 6-Formylindolo [3, 2-b] carbazole, a potent ligand for the aryl hydrocarbon receptor produced both endogenously and by microorganisms, can either promote or restrain inflammatory responses. *Front. Toxicol.* **2022**, *4*, 775010.

(84) Zhao, C.; Bao, L.; Qiu, M.; Feng, L.; Chen, L.; Liu, Z.; Duan, S.; Zhao, Y.; Wu, K.; Zhang, N.; Hu, X.; Fu, Y. Dietary tryptophan-mediated aryl hydrocarbon receptor activation by the gut microbiota alleviates escherichia coli-induced endometritis in mice. *Microbiol. Spectr.* **2022**, *10*, e0081122.

(85) Justiniano, R.; de Faria Lopes, L.; Perer, J.; Hua, A.; Park, S. L.; Jandova, J.; Baptista, M. S.; Wondrak, G. T. The endogenous tryptophan-derived photoproduct 6-formylindolo[3,2-b]carbazole (FICZ) is a nanomolar photosensitizer that can be harnessed for the photodynamic elimination of skin cancer cells in vitro and in vivo. *Photochem. Photobiol.* **2021**, *97*, 180-191.

(86) Vincent, F.; Nueda, A.; Lee, J.; Schenone, M.; Prunotto, M.; Mercola, M. Phenotypic drug discovery: recent successes, lessons learned and new directions. *Nat. Rev. Drug Discov.* **2022**, *21*, 899-914.

(87) Moffat, J. G.; Vincent, F.; Lee, J. A.; Eder, J.; Prunotto, M. Opportunities and challenges in phenotypic drug discovery: an industry perspective. *Nat. Rev. Drug Discov.* **2017**, *16*, 531-543.

(88) Barbato, L.; Bocchetti, M.; Di Biase, A.; Regad, T. Cancer stem cells and targeting strategies. *Cells* **2019**, *8*, 926.

(89) Ju, F.; Atyah, M. M.; Horstmann, N.; Gul, S.; Vago, R.; Bruns, C. J.; Zhao, Y.; Dong, Q. Z.; Ren, N. Characteristics of the cancer stem cell niche and therapeutic strategies. *Stem Cell Res. Ther.* **2022**, *13*, 233.

(90) Vessoni, A. T.; Filippi-Chiela, E. C.; Lenz, G.; Batista, L. F. Z. Tumor propagating cells: drivers of tumor plasticity, heterogeneity, and recurrence. *Oncogene* **2020**, *39*, 2055-2068.

(91) Vetrie, D.; Helgason, G. V.; Copland, M. The leukaemia stem cell: similarities, differences and clinical prospects in CML and AML. *Nat. Rev. Cancer* **2020**, *20*, 158-173.

(92) López-Rodríguez, M. L.; Benhamú, B.; Vázquez-Villa, H.; Algar, S.; Sánchez-Merino, A.; Gallardo, M. NPM1-depending leukemia agents. Patent PCT/EP2022/076831, WO2023/0523542021.

(93) Li, Y.; Oo, Z. Y.; Chang, S. Y.; Huang, P.; Eng, K. G.; Zeng, J. L.; Kaestli, A. J.; Gopalan, B.; Kandasamy, K.; Tasnim, F.; Zink, D. An in vitro method for the prediction of renal proximal tubular toxicity in humans. *Toxicol. Res.* **2013**, *2*, 352-365.

(94) Tiong, H. Y.; Huang, P.; Xiong, S.; Li, Y.; Vathsala, A.; Zink, D. Drug-induced nephrotoxicity: clinical impact and preclinical in vitro models. *Mol. Pharm.* **2014**, *11*, 1933-1948.

(95) Liu, Y.; Nappi, M.; Arceo, E.; Vera, S.; Melchiorre, P. Asymmetric catalysis of Diels-Alder reactions with in situ generated heterocyclic ortho-quinodimethanes. *J. Am. Chem. Soc.* **2011**, *133*, 15212-15218.

(96) Szcześniak, P.; Staszewska-Krajewska, O.; Furman, B.; Młynarski, J. Asymmetric synthesis of cyclic nitrones via organocatalytic michael addition of aldehydes to nitroolefins and subsequent reductive cyclization. *ChemistrySelect* **2017**, *2*, 2670-2676.

(97) Möhler, J. S.; Schnitzer, T.; Wennemers, H. Amine catalysis with substrates bearing N-heterocyclic moieties enabled by control over the enamine pyramidalization direction. *Chem. - Eur. J.* **2020**, *26*, 15623-15628.

(98) Yato, M.; Homma, K.; Ishida, A. Reduction of carboxylic esters to ethers with triethyl silane in the combined use of titanium tetrachloride and trimethylsilyl trifluoromethanesulfonate. *Tetrahedron* **2001**, *57*, 5353-5359.

(99) Bajwa, J. S.; Jiang, X.; Slade, J.; Prasad, K.; Repič, O.; Blacklock, T. J. In-situ generation of Et_3SiBr from $BiBr_3$ and Et_3SiH and its use in preparation of dialkyl ethers. *Tetrahedron Lett.* **2002**, *43*, 6709-6713.

(100) Zhao, C.; Sojdak, C. A.; Myint, W.; Seidel, D. Reductive etherification via anion-binding catalysis. *J. Am. Chem. Soc.* **2017**, *139*, 10224-10227.

(101) Hatakeyama, S.; Mori, H.; Kitano, K.; Yamada, H.; Nishizawa, M. Efficient reductive etherification of carbonyl compounds with alkoxytrimethylsilanes. *Tetrahedron Lett.* **1994**, *35*, 4367-4370.

(102) Dueno, E. E.; Chu, F.; Kim, S.-I.; Jung, K. W. Cesium promoted O-alkylation of alcohols for the efficient ether synthesis. *Tetrahedron Lett.* **1999**, *40*, 1843-1846.

(103) Salvatore, R. N.; Nagle, A. S.; Schmidt, S. E.; Jung, K. W. Cesium hydroxide promoted chemoselective N-alkylation for the generally efficient synthesis of secondary amines. *Org. Lett.* **1999**, *1*, 1893-1896.

(104) *TRANSIL HSA binding kit*. https://sovicell.com/products/tpb-0210-2096 (accessed 02 July 2024).

(105) Dhayalan, V.; Clement, J. A.; Jagan, R.; Mohanakrishnan, A. K. A versatile synthesis of annulated carbazole analogs involving a domino reaction of bromomethylindoles with arenes/heteroarenes. *Eur. J. Org. Chem.* **2009**, *2009*, 531-546.

(106) Mital, A.; Murugesan, D.; Kaiser, M.; Yeates, C.; Gilbert, I. H. Discovery and optimisation studies of antimalarial phenotypic hits. *Eur. J. Med. Chem.* **2015**, *103*, 530-538.

(107) Zhang, M.; Hu, P.; Zhou, J.; Wu, G.; Huang, S.; Su, W. Pd-catalyzed multidehydrogenative cross-coupling between (hetero) arenes and nitroethane to construct β-aryl nitroethylenes. *Org. Lett.* **2013**, *15*, 1718-1721.

(108) Sathish, M.; Chetna, J.; Hari Krishna, N.; Shankaraiah, N.; Alarifi, A.; Kamal, A. Iron-mediated one-pot synthesis of 3, 5-diarylpyridines from β-nitrostyrenes. *J. Org. Chem.* **2016**, *81*, 2159-2165.

(109) Ambala, S.; Singh, R.; Singh, M.; Cham, P. S.; Gupta, R.; Munagala, G.; Yempalla, K. R.; Vishwakarma, R. A.; Singh, P. P. Metal-free, room temperature, acid-$K_2S_2O_8$ mediated method for the nitration of olefins: an easy approach for the synthesis of nitroolefins. *RSC Adv.* **2019**, *9*, 30428-30431.

(110) Thanetchaiyakup, A.; Rattanarat, H.; Chuanopparat, N.; Ngernmeesri, P. One-pot synthesis of substituted indolo [1,2-a] quinolines under transition-metal-free conditions. *Tetrahedron Lett.* **2018**, *59*, 1014-1018.